Breakdown Voltage of Compressed Sulfur Hexafluoride (SF_6)

at Very Low Frequency / Low Frequency (30 kHz)

by

Jian Han

A Thesis Presented in Partial Fulfillment
of the Requirements for the Degree
Master of Science

Approved October 2010 by the
Graduate Supervisory Committee:

Ravi S. Gorur, Chair
Richard G. Farmer
George G. Karady

ARIZONA STATE UNIVERSITY

December 2010

ABSTRACT

The U.S. Navy is interested in evaluating the dielectric performance of SF_6 at 30 kHz in order to develop optimal bushing designs and to ensure reliable operation for the Very Low Frequency/ Low Frequency (VLF/LF) transmitting stations. The breakdown experiments of compressed SF_6 at 30 kHz in the pressure range of 1-5 atm were conducted in both the uniform field (plane-plane gap) and the non-uniform field (rod-plane gap). To understand the impact of pressure on the breakdown voltage of SF_6 at VLF/LF, empirical models of the dielectric strength of SF_6 were derived based on the experimental data and regression analysis. The pressure correction factors that present the correlation between the breakdown voltage of SF_6 at VLF/LF and that of air at 50/60 Hz were calculated. These empirical models provide an effective way to use the extensively documented breakdown voltage data of air at 60 Hz to evaluate the dielectric performance of SF_6 for the design of VLF/LF high voltage equipment. In addition, several breakdown experiments and similar regression analysis of air at 30 kHz were conducted as well. A ratio of the breakdown voltage of SF_6 to that of air at VLF/LF was calculated, from which a significant difference between the uniform gap and the non-uniform gap was observed. All the models and values provide useful information to evaluate and predict the performance of the bushings in practice.

TABLE OF CONTENTS

Page

LIST OF TABLES

LIST OF FIGURES

CHAPTER 1

INTRODUCTION

The U.S. Navy operates several VLF/LF transmitters to communicate with submarines. By definition, VLF covers the frequency range from 3-30 kHz and LF covers the frequency range from 30-300 kHz. VLF/LF supports long-distance communication because the ionosphere aids in radio wave refraction and propagation is not greatly affected by solar flares. The ability of VLF/LF to penetrate seawater allows communication with fully submerged submarines [1].

These transmitters operate in the range of 150-300 kV and connect to outdoor antennae through bushings pressurized with SF_6 gas. The electrical performance of the bushings is an important factor in the reliable operation of VLF/LF transmitters. The rated pressure of SF_6 in the bushings is 5 atm. Since leakage of the gas is a possibility, the pressure will in practice may be less than 5 atm. The dielectric performance of the bushings is a function of the pressure of the SF_6. The U.S. Navy is interested in evaluating the dielectric performance of SF_6 at 30 kHz in order to develop optimal bushing designs and ensure reliable operation for the VLF/LF transmitting stations.

Motivated by the demand of electric power industry development, there are adequate literatures describing dielectric characteristic of SF_6 under DC and 50/60 Hz [2]-[8]. Since outdoor insulation need to stand for lightning strikes, dielectric property of SF_6 under standard impulse also been investigated [9]-[12]. In addition, several experiments at High Frequency (HF) in MHz range have been conducted. Most of them tested the dielectric characteristic of compressed gas up to 1 atm pressure [13]-[15].

To obtain economical insulation with optimal dielectric property, the dielectric properties of the SF_6-gas mixture have attracted lots of attends [16]-[18]. Reference [17] provides comprehensive review of experimental investigations about the SF_6 mixed with various gases.

Recently, a high voltage and insulation group at Tokyo Electric Power Company completed a series of experiments to study the breakdown characteristics of SF_6 for non-standard lightning impulse waves associated with lightning surges and disconnector switching surges [19]-[22]. The breakdown voltage over time characteristic of SF_6 gap at a pressure of 0.5 MPa pressure was analyzed.

However, little information is available regarding the breakdown characteristic of SF_6 at VLF/LF, this special-purpose radio frequency range. The dielectric properties of SF_6 are significantly different over the frequency ranges investigated. Therefore it is important to evaluate the dielectric performance of SF_6 at VLF/LF. This paper describes the results of high voltage breakdown experiments of SF_6 at 30 kHz with the pressure varied between 1-5 atm. In addition, since the breakdown characteristics of air at power frequency have been extensively documented, it is of practical interest to correlate the breakdown voltage of SF_6 at VLF/LF with that of air at 50/60 Hz or 30 kHz. In order to do this, several breakdown experiments of air at 60 Hz and 30 kHz were conducted. The comparison of dielectric strength between SF_6 and air at VLF/LF provides useful information to evaluate and predict the performance of the bushings.

CHAPTER 2

DESCRIPTION OF EXPERIMENT

Test Facility

Chamber

All experiments were conducted in a cylindrical metal chamber with height 60 cm, and diameter 50 cm, as shown in Fig. 1 (a). The body of the chamber was made from aluminum and end caps made from stainless steel. Flanges with O-sealing rings between body and end caps guarantee the leak tightness of the chamber. The breakdown phenomena can be observed from two viewing windows at the side. Another window that can be opened was used for changing electrodes. The upper electrode was connected to high voltage supply through a partial discharge (PD) free bushing rated for 100 kV. The lower electrode was connected to the bottom of the chamber through a screw that is capable of changing the gap length between two electrodes. The lower electrode and the chamber body were grounded. Two valves were installed at the bottom, one for pumping test gas into the chamber and the other for deflating and vacuumization. A digital pressure gauge connected to the bottom measures the instantaneous pressure within the chamber. The chamber was evacuated to absolute pressure less than 0.02 atm (1.5 kPa) before being filled with the test gas. The air and SF_6 used were of commercial purity. To investigate the gaseous breakdown voltage under uniform and very non-uniform electric fields, plane-plane and rod-plane electrode configurations were used, respectively, as shown in Fig. 1 (b), and (c).

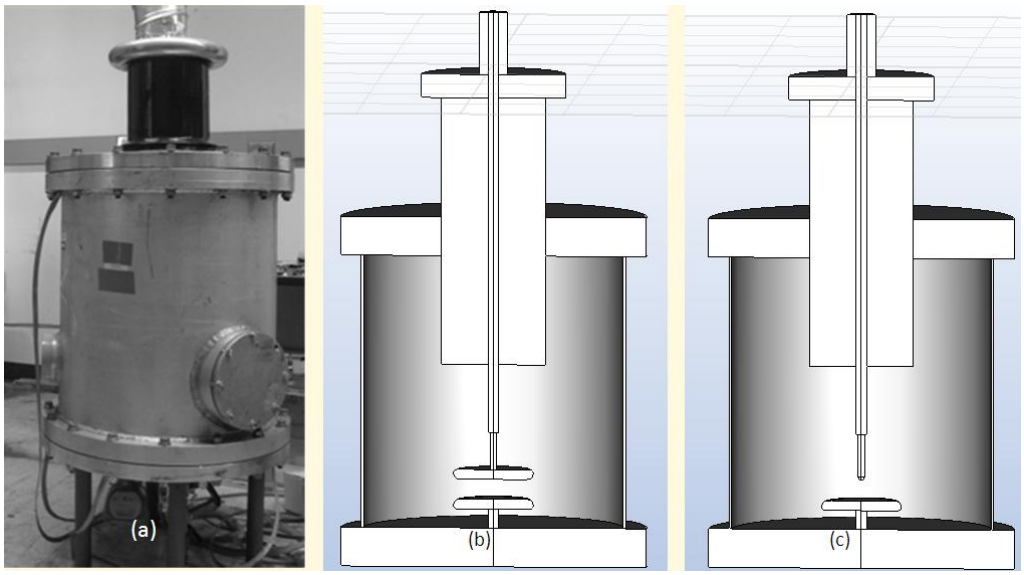

Fig. 1 (a) Metal chamber (b) Schematic for plane-plane electrode configuration (c) Schematic for rod-plane electrode configuration

Electrodes

All the electrodes, as shown in Fig. 2 (a), were made of stainless steel as they do not react with air or SF_6 and are also resistant to sparks caused by breakdown. Previous experiment verified that no marked difference was observed in SF_6 breakdown property for different electrode materials [4].

The rod electrode had a length of 81 mm with a hemispherical tip 13 mm in diameter. The plane electrode was 150 mm diameter and was shaped to the Rogowski profile. The ideal uniform electric field requires the plane electrode to have infinite dimension, which is practically impossible to meet. The Rogowski profile can reduce the high field at the edges of finite sized plane electrode, in order to produce the uniform electric field.

Uniform electric field also attributes to the parallelism of two plane electrodes. A special connector was designed to keep the two plane electrodes paralleling with each other. As shown in Fig. 2 (b), three screws through the connector match with the screw thread on the back of the plane electrode. One spring is positioned between the connector and the plane electrode. By adjusting these screws, the balance between the gravity of the electrode and the compressive force of the spring makes two plane electrodes parallel. Since the relative parallel property is of interest, it is more efficient to adjust the upper one keeping the lower electrode fixed.

(a)

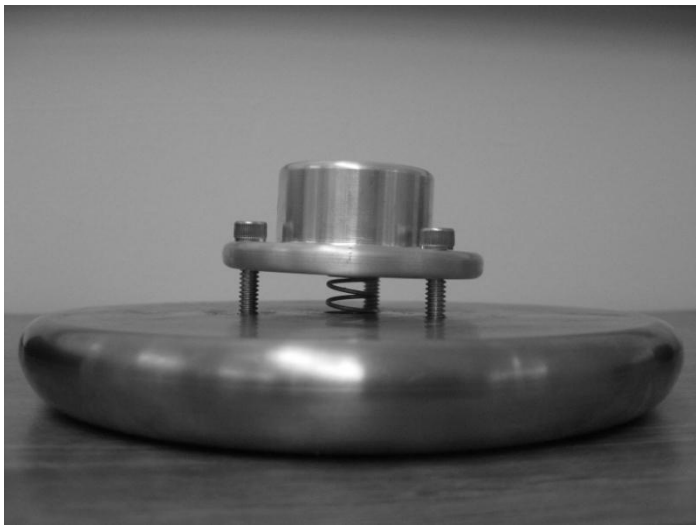

(b)

Fig. 2 Electrode configuration (a) plane and rod electrode (b) plane electrode with connection components

Experimental setting at Edgar Beauchamp High Voltage Test Facility (EBHVTF)

The 30 kHz measurements were performed at the Edgar Beauchamp High Voltage Test Facility (EBHVTF) of the U.S. Navy (California).The power supply consists of a Westinghouse (AN/FRA-31) 100-kW VLF/LF transmitter with a helical coil and capacitor stack forming a resonant circuit, as shown in Fig.3. The helix is a large air-wound solenoid coil with adjustable inductance up to 14.6 mH. The capacitor stack is in series-parallel combination. The resonant tank circuit can generate voltages up to 250 kV_{rms}.

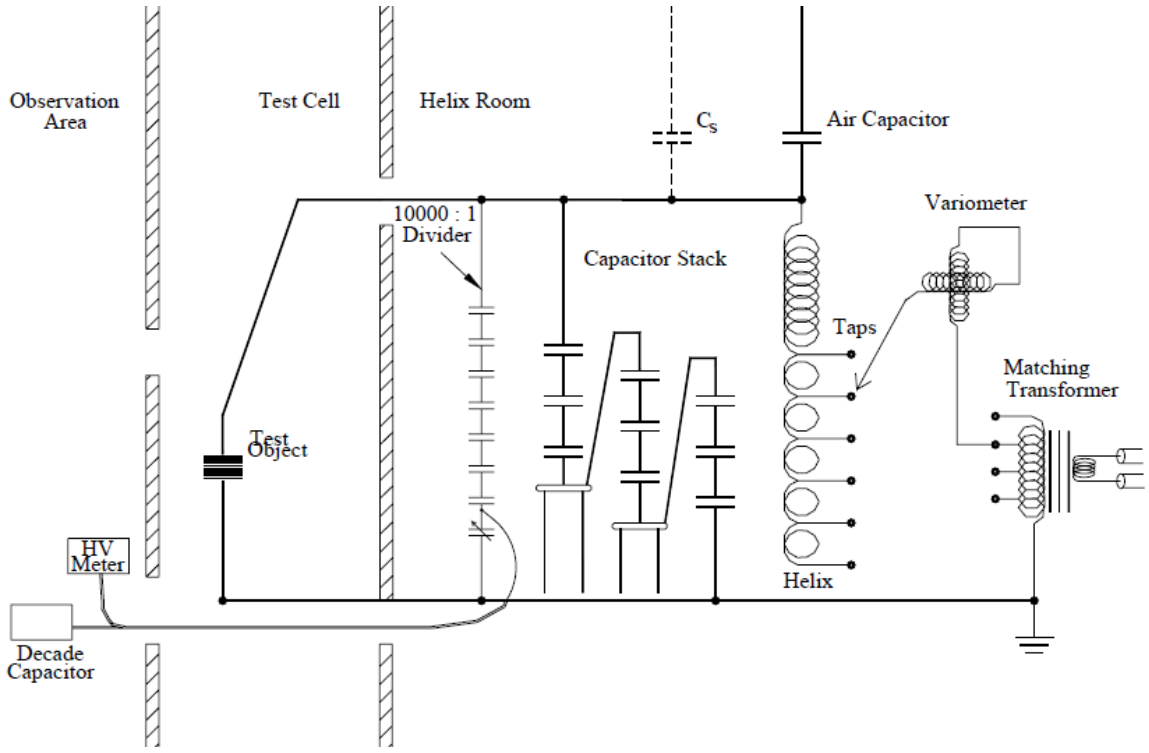

Fig.3 Schematic of experiment setting at Dixon [1]

Experiment setting at Arizona State University (ASU)

The compressed air breakdown experiments at 60 Hz were performed at ASU The facility at the roof of Engineering Research Center is capable of providing high voltage up to 100 kV at 60 Hz. The experimental setting is demonstrated in Fig.4.

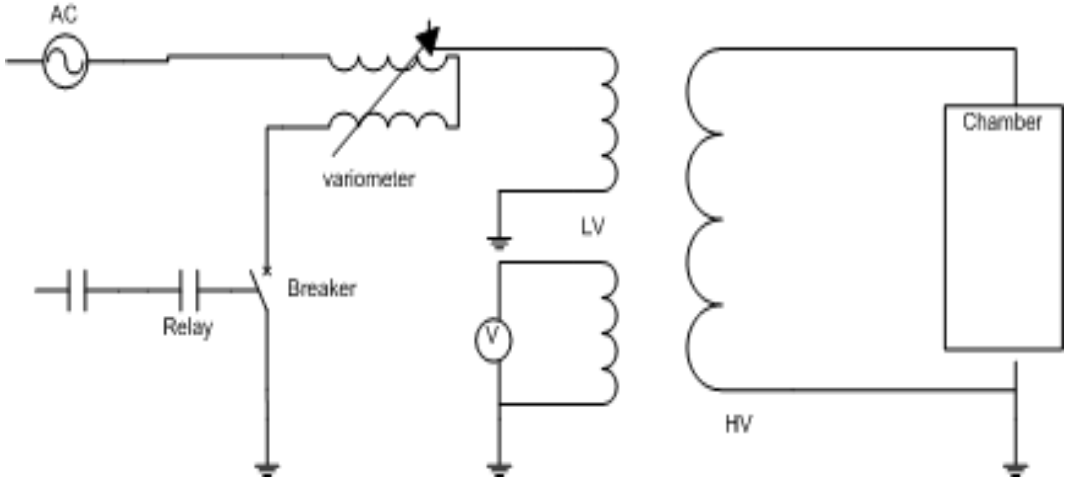

Fig.4 Schematic of experiment setting at ASU

The entire setting consisted of a protection circuit, a 0-100 kV transformers and supply pipes. The protection circuit included one circuit breaker and two in series cooperated relays. One relay was installed at the door of a cage. The cage protected the operator from the high voltage experiment. The other one was controlled by the safety button. If flashover or other emergency occurs, the operator can push the button to cut off the power supply to the whole circuit. Only when the cage door was fully closed and the safety button was in the released position, the 60 Hz, 110 Volts power can be supplied. A wheel variometer was connected between the power supply and the transformer, to control the voltage at the lower side of the transformer. This single phase potential transformer was manufactured by Westinghouse with two optional ratios, 600:1 and 1000:1. To apply higher voltage on the tested gap, the ratio 1000:1 was selected for all

the experiment. The aluminum pipes distributed power from the high voltage end of transformer to the upper electrode in the chamber. The usage of aluminum pipe can eliminate corona which would occur on wires if used, when voltage was greater than 60 kV.

Experiment Procedure

30 kHz breakdown procedure

1) Set up the test chamber and check the leak tightness.
2) Adjust the transmitter frequency to the value where maximum voltage occurs in the high voltage tuned circuit.
3) Use Jennings voltage divider and 10000:1 voltage divider to calibrate.
4) Set the gap length by using gauge blocks
5) Make the two plane electrodes parallel by adjusting screws if uniform gap is tested.
6) Clean the electrode surface with alcohol.
7) Fill the chamber with tested gas and complete breakdown experiment (detailed process will be discussed later).

These processes below are applicable to SF_6 breakdown experiment only

8) Use a vacuum pump to evacuate the chamber to the absolute pressure less than 0.02 atm (1.5 kPa).
9) Fill in the chamber with SF_6 gas to 1 atm pressure and complete breakdown experiments at one setting gap length.

10) Keep this gap length and compress the chamber to 2 atm without releasing previous SF_6 gas and complete all breakdown experiments.
11) Continue the same process to complete all breakdown experiments with pressure from 3 atm to 5 atm.
12) Recycle the tested SF_6 gas in special container after finishing experiments at 5 atm.
13) Change the gap length and repeat these steps above.

The reason behind filling more gas in the chamber without releasing the originally tested gas (rather than evacuating the chamber and refilling with fresh gas) is that the SF_6 deterioration has ignorable influence on its breakdown voltage. Although there are byproducts after flashover, most of them recombine to reform SF_6 quickly. The recovery ability makes SF_6 an excellent insulation gas. As the new filled gas decreases the byproducts percentage among all the SF_6 gas, it helps to reduce the deterioration effect. Less than 10 flashovers were conducted for a certain combination of gap length and pressure. The deterioration effect is limited by the relatively few times of flashover. The tight time schedule given to conduct these experiments is another reason. All the breakdown experiments were planned to finish within a week. The vaccumization and pressurization are time consuming processes. If SF_6 is changed after one certain combination of gap and pressure testing, it will take much longer time.

The experimental data finally proved that this process is acceptable. The last 5 breakdown voltages for the largest plane-plane and rod-plane gap from 1 to 5 atm in time order are plotted in Fig.5 and Fig.6 respectively. The random patterns indicate neglectable deterioration effect on SF_6 dielectric strength. An obvious decreasing trend of

breakdown voltage with time order should be observed, if deterioration effect is significant.

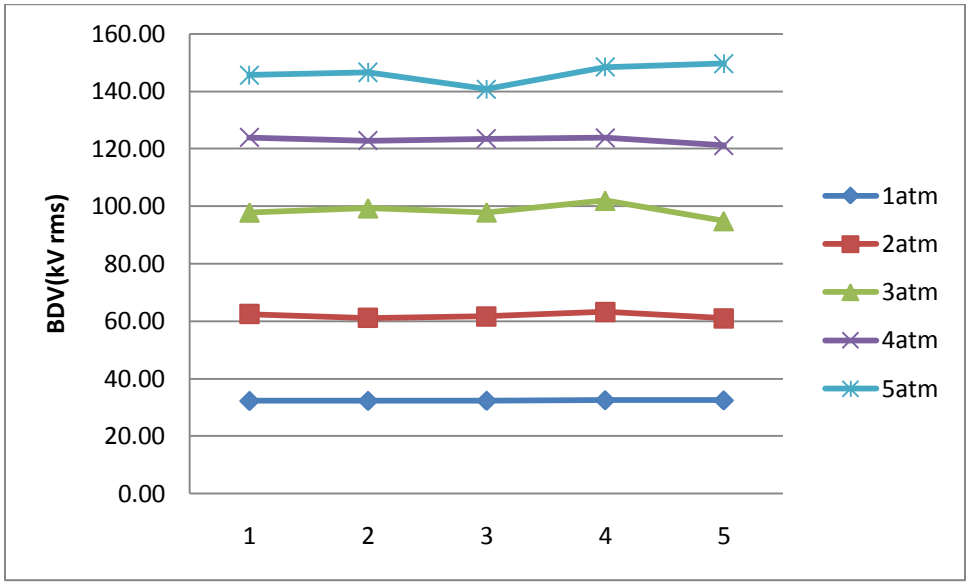

Fig.5 Breakdown voltage of 5 mm plane-plane SF_6 gap in time order at 30 kHz

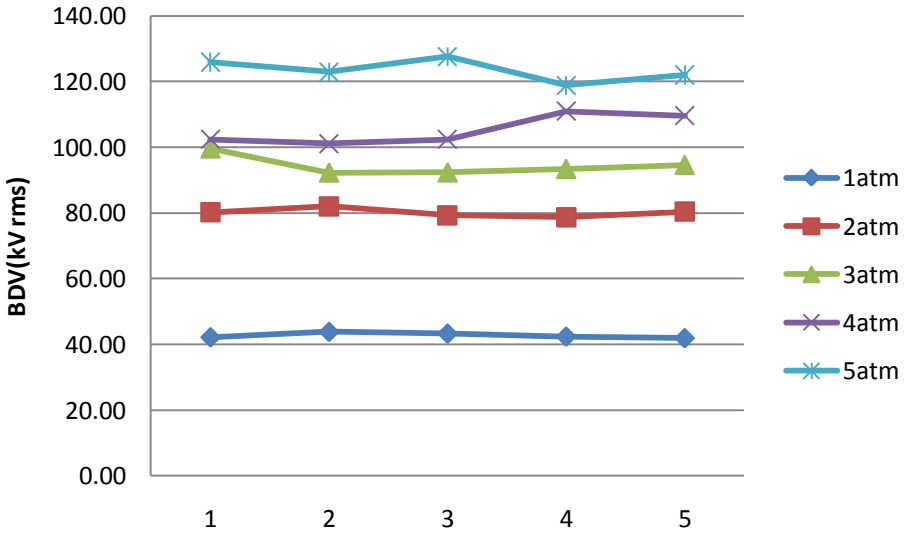

Fig.6 Breakdown voltage of 15 mm rod-plane SF_6 gap in time order at 30 kHz

Important annotations about experiments

1) Detection of stationary corona

Corona cameras are not able to detect corona in the chamber. No visual corona phenomena can be observed from cameras, since both the chamber made of metal and the view windows made of plexiglass block the spectrum. Alternatively, the use of oscilloscope is an effective way to indirectly detect corona. Current through the grounding braid is measured by a current transformer and converted to voltage signal as the input to the oscilloscope. The waveform shown on oscilloscope is sinusoid and the magnitude proportionally increases with the applied voltage until corona occurs. A ripple at the peak or trough of sinusoidal wave implies existence of corona. The impact of corona on the grounding current leads to this distortion of the wave. Since no obvious distortion of waveform was observed in all of the experimental scenarios, we conclude that no corona happened prior to flashover.

2) Requirements for valid breakdown experiment

According to IEEE standards, time interval for a valid experiment should be between 5 to 15 seconds. By definition, the time interval starts when voltage is applied and ends when flashover occurs. The initial applied voltage and the ramp rate are the two important parameters together determining the time interval. The ramp rate indicates how fast the applied voltage increases. The time interval becomes shorter if the initial voltage is higher and/or the ramp rate rises up. The operator should set proper value in the computer program to control the transmitter, in order to make the time interval satisfy the requirement.

At least five replicates should be conducted and the last five qualified replicates are selected for data analysis. The qualified replicates should have the characteristics that no specific pattern shows in the breakdown voltage vs. time order, and the ratio of standard deviation to the average is less than 10%. These requirements can reduce the effect led by assignable causes. Considering that the initial applied voltage and the ramp rate are the parameters set by computer program, there should be no dramatic variation of breakdown voltage among the replicates. If one flashover happens much faster than previous, it is possible that unusual cause drives this flashover and the accuracy of this breakdown voltage would be highly suspected.

3) The Real Breakdown Voltage

The real breakdown voltage was the voltage meter reading multiplied by the atmospheric correction factors and calibration ratio. The atmospheric correction factors contain density correction factor and humidity correction factors, regulated in IEEE standards [23], [24]. For the air breakdown experiment at 1 atm, both two factors should be considered because the electrodes were in ambient environment. For air breakdown experiment beyond 1 atm and all SF_6 experiments, only the modified density correction was applied. The chamber isolates the test gas from the ambient environment. The test gas is industrial dry gas. Therefore, the humidity and ambient pressure fluctuations have neglectable effect on experimental results. However, temperature should be taken into consideration, since experiment takes a relatively long time and the metal chamber is a good heat conductor. Modified density correction factor is a function of the temperature shown in Equation (1)

$$k = \frac{273 + t_0}{273 + t} \tag{1}$$

where t denotes ambient temperate in degree Celsius

$$t_0 = 20\ ^oC \tag{2}$$

The purpose of calibration is to get the ratio of the voltage meter measurement to the real applied voltage. The process of calibration for VLF/LF at Dixon is complicated since the high voltage is generated by the resonance circuit. The combination of the Jennings bottle divider and the 10000:1 divider is necessary. The setting at ASU makes the calibration simplified. The voltage meter M1 measured the applied voltage cross the test gas gap. The voltage meter M2 was used to measure the voltage at the secondary side of transformer. Limit the applied voltage within the range of both meters and simultaneously record the readings. After five pairs of readings were collected for one applied voltage, the ratio of each pair was calculated. The average of all the ratios was the final calibration. To increase the accuracy, the applied voltages were changed randomly and the procedure was repeated. Table 1 and Fig.7 indicate that the ratio is independent of the applied voltage and match with the rated ratio marked on the transformer plate.

Table 1

Reading of Voltage Meters and the Calibration Ratio

M1 reading (V rms)	M2 reading (V rms)	M1/M2
278.96	0.2761	1010.36
367.63	0.3635	1011.36
369.71	0.3659	1010.41
443.02	0.4406	1005.49
663.20	0.6589	1006.53
821.21	0.8165	1005.76

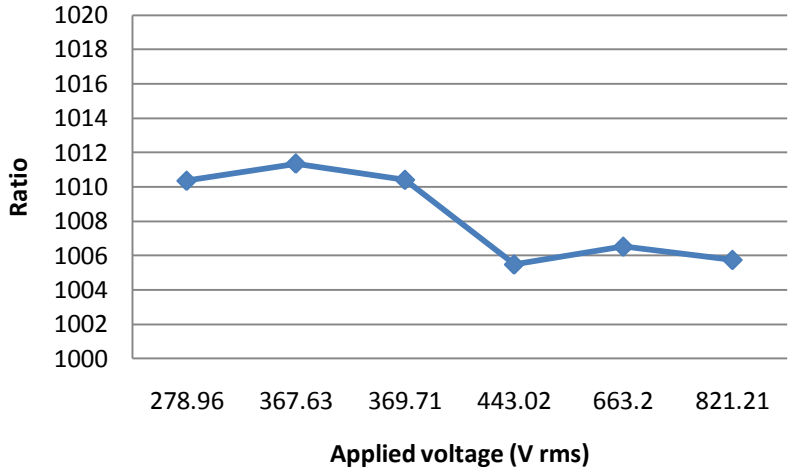

Fig.7 Relationship between calibration ratio and the applied voltage

CHAPTER 3

EXPERIMENTAL RESULTS AND DISCUSSION

Experimental Results

Table 2 shows the summary of tests performed. The gap lengths tested were 2.5 mm and 5 mm for uniform field gap, and 8 mm and 15 mm for non-uniform field gap. At each gap, the pressure was set from varied 1 atm to 5 atm using 1 atm increment. All SF_6 breakdown experiments were carried out at 30 kHz.

Table 2

Summary of the experiments conducted

Gas	Gap configuration	Pressure (atm)	Gap length (mm)	Frequency
SF_6	Plane-Plane	1, 2, 3, 4, 5	2.5, 5	30 kHz
SF_6	Rod-Plane	1, 2, 3, 4, 5	8, 15	30 kHz
Air	Plane-Plane	1, 2, 3, 4, 5	5	30 kHz
Air	Rod-Plane	1, 2, 3, 4, 5	15	30 kHz
Air	Plane-Plane	1, 2, 3, 4, 5	2.5, 5	60 Hz
Air	Rod-Plane	1, 2, 3, 4, 5	8, 15	60 Hz

Since corona was not observed before flashover in all the tests, breakdown voltage is of most interest in the dielectric property study. As mentioned in previous chapters, the real breakdown voltages of last five or ten valid flashover replicates were calculated using the voltage meter readings multiplied by the calibration and correction factors. Table 3-Table 7 demonstrate all the breakdown voltage of various gaps. The table heading describes the gap length and pressure. The valid replicated breakdown voltages

are listed in time order. For each test scenario, the average and standard deviation are calculated, denoted as AVE and STD in the tables. The ratio of standard deviation to the average indicates the fluctuation among the series breakdown voltages.

Table 3

Breakdown voltage of SF_6 plane-plane gap at 30 kHz

Test #	Breakdown voltage (kV rms)									
	2.5 mm gap length					5 mm gap length				
	1 atm	2 atm	3 atm	4 atm	5 atm	1 atm	2 atm	3 atm	4 atm	5 atm
1	15.91	33.90	53.62	72.79	94.21	32.26	62.45	97.83	123.93	145.66
2	15.96	34.60	54.63	70.76	92.55	32.28	61.13	99.29	122.84	146.60
3	15.77	35.11	51.20	73.58	94.77	32.32	61.70	97.87	123.53	140.68
4	15.83	32.81	53.55	71.78	93.00	32.52	63.26	101.93	123.79	148.40
5	15.56	32.89	53.72	70.71	94.37	32.45	60.96	94.84	121.12	149.63
AVE	15.81	33.86	53.34	71.92	93.78	32.37	61.90	98.35	123.04	146.19
STD	0.15	1.02	1.28	1.26	0.96	0.11	0.96	2.58	1.15	3.45
STD/AVE	0.97%	3.01%	2.39%	1.75%	1.02%	0.35%	1.55%	2.62%	0.94%	2.36%

Table 4

Breakdown voltage of SF_6 rod-plane gap at 30 kHz

Test #	Breakdown voltage (kV rms)									
	8 mm gap length					15 mm gap length				
	1 atm	2 atm	3 atm	4 atm	5 atm	1 atm	2 atm	3 atm	4 atm	5 atm
1	33.26	64.38	84.43	92.61	109.80	42.17	80.15	99.60	102.42	125.94
2	38.33	67.35	86.62	87.53	102.78	43.79	82.01	92.30	101.10	122.98
3	36.60	66.24	82.06	100.70	106.12	43.27	79.29	92.34	102.36	127.61
4	37.47	59.74	81.81	93.87	111.29	42.35	78.68	93.39	110.95	118.86
5	33.35	61.71	89.73	89.08	104.14	41.89	80.37	94.62	109.63	122.03
AVE	35.80	63.88	84.93	92.76	106.82	42.69	80.10	94.45	105.29	123.48
STD	2.36	3.15	3.32	5.13	3.64	0.80	1.26	3.03	4.62	3.42
STD/AVE	6.59%	4.93%	3.91%	5.53%	3.40%	1.88%	1.58%	3.21%	4.38%	2.77%

Table 5

Breakdown voltage of air plane-plane and rod-plane gap at 30 kHz

Test #	Breakdown voltage (kV rms)									
	5 mm plane-plane gap					15 mm rod-plane gap				
	1 atm	2 atm	3 atm	4 atm	5 atm	1 atm	2 atm	3 atm	4 atm	5 atm
1	11.89	23.00	35.73	45.18	61.42	19.68	35.20	49.28	60.64	66.83
2	11.89	23.04	35.73	47.22	63.68	19.22	34.25	47.14	59.19	66.45
3	11.97	22.80	36.55	49.13	64.21	19.89	35.54	44.35	60.79	66.12
4	12.10	22.25	35.73	49.10	60.38	18.91	34.60	47.06	58.69	67.82
5	11.94	23.03	35.72	47.31	60.35	19.64	34.70	49.54	59.20	69.27
AVE	11.96	22.82	35.89	47.59	62.01	19.47	34.86	47.47	59.70	67.30
STD	0.09	0.33	0.37	1.63	1.83	0.40	0.51	2.10	0.95	1.27
STD/AVE	0.73%	1.46%	1.03%	3.43%	2.95%	2.03%	1.46%	4.42%	1.58%	1.89%

Table 6

Breakdown voltage of air rod-plane gap at 60 Hz

Test #	Breakdown voltage (kV rms)									
	8 mm gap length					15 mm gap length				
	1 atm	2 atm	3 atm	4 atm	5 atm	1 atm	2 atm	3 atm	4 atm	5 atm
1	16.38	27.48	40.63	52.51	66.43	19.70	37.49	51.07	63.33	75.16
2	15.71	25.62	38.89	50.47	66.41	19.83	34.15	50.86	62.34	75.31
3	16.58	27.81	39.95	54.54	63.98	18.60	35.36	49.92	62.83	75.92
4	16.49	29.85	40.91	54.23	67.19	19.93	36.49	52.08	63.85	76.24
5	16.87	27.26	38.93	52.62	66.49	19.41	36.45	53.09	63.23	75.55
6	17.08	27.19	40.90	48.43	66.00	19.91	37.36	51.47	64.02	75.73
7	15.78	29.83	41.34	54.51	65.47	20.37	36.14	50.01	64.31	74.46
8	15.64	28.86	40.17	52.51	65.39	20.12	36.85	51.11	64.43	75.81
9	16.48	26.72	41.10	54.77	65.26	19.73	37.29	51.82	63.16	75.91
10	16.88	27.09	39.11	51.67	65.54	19.63	37.18	53.15	63.84	76.60
AVE	16.39	27.77	40.19	52.62	65.82	19.72	36.48	51.46	63.53	75.67
STD	0.52	1.36	0.94	2.04	0.89	0.48	1.05	1.11	0.67	0.59
STD/AVE	3.15%	4.90%	2.33%	3.88%	1.36%	2.41%	2.88%	2.16%	1.05%	0.79%

Table 7

Breakdown voltage of air plane-plane gap at 60 Hz

Test #	Breakdown voltage (kV rms)									
	2.5 mm gap length					5 mm gap length				
	1 atm	2 atm	3 atm	4 atm	5 atm	1 atm	2 atm	3 atm	4 atm	5 atm
1	5.80	11.26	22.10	31.80	41.21	11.13	21.48	34.68	48.28	59.16
2	5.85	11.12	21.72	32.54	41.12	10.80	21.68	35.12	47.45	61.86
3	5.93	11.09	21.62	32.62	41.20	11.02	22.09	34.83	47.43	60.72
4	5.86	11.70	22.16	32.64	42.41	10.88	22.31	32.98	44.28	61.97
5	5.87	11.77	22.17	32.75	41.87	11.04	22.33	35.51	46.90	59.90
6	5.86	11.10	21.66	33.44	42.23	10.99	22.83	35.33	46.70	62.44
7	5.88	11.18	22.12	31.90	42.41	10.93	22.74	35.37	49.31	62.46
8	6.00	11.08	22.19	32.48	40.96	10.97	21.79	34.26	49.21	61.89
9	5.86	11.77	21.77	33.05	41.83	11.07	22.07	33.21	48.81	60.99
10	5.83	11.80	21.64	32.26	42.55	10.97	22.82	35.76	47.11	63.39
AVE	5.87	11.39	21.91	32.55	41.78	10.98	22.21	34.71	47.55	61.48
STD	0.06	0.33	0.25	0.49	0.61	0.09	0.48	0.95	1.49	1.28
STD/AVE	0.94%	2.88%	1.14%	1.51%	1.46%	0.86%	2.17%	2.74%	3.14%	2.08%

Validation of the Experimental Phenomena and Results

No sustained corona was observed before flashover for tested SF_6 gaps

The diameter of the rod electrode is one of the main reasons. As shown in Fig.8 with an increase in the diameter of rod electrode, the first phase of breakdown voltage decreases before extreme value occurs, and corona onset voltage increases [25]. Therefore, the difference between the breakdown voltage and the corona onset voltage is

smaller for a larger diameter rod electrode. The pressure value where the corona onset voltage overlaps with breakdown voltage is denoted as critical pressure. The critical pressure becomes smaller as rod diameter increases. For rod electrode with a diameter of 12.6 inches, the critical pressure is close to 1 atm.

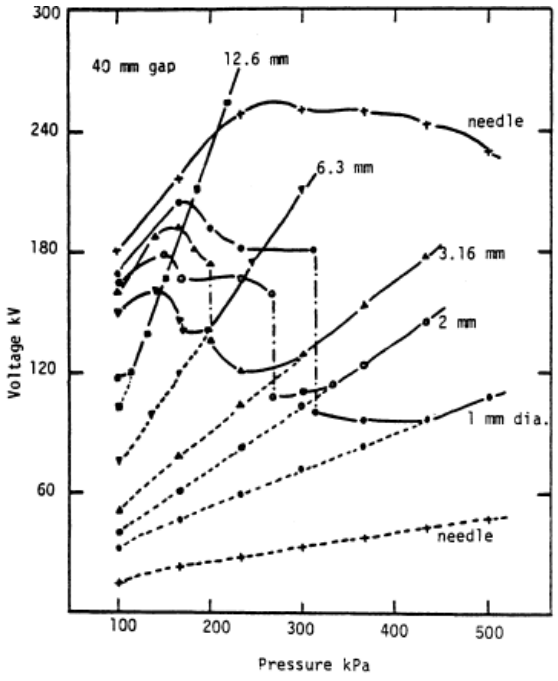

Fig.8 Effect of the rod diameter on the breakdown voltage-pressure characteristics of rod-plane SF_6 gap [25]

Gap length is another factor that contributes to no corona observed before breakdown. As shown in Fig.9, the shorter gap corresponds to the lower critical pressure. Compared with the corona onset voltage and breakdown voltage at the same pressure with different gap length, the smaller the gap is, the corona onset voltage and the breakdown voltage are closer to the same value. When the gap is 20 mm, there is no corona before breakdown at pressures higher than 2 atm, and the maximum difference between breakdown voltage and corona onset voltage is only round 20 kV.

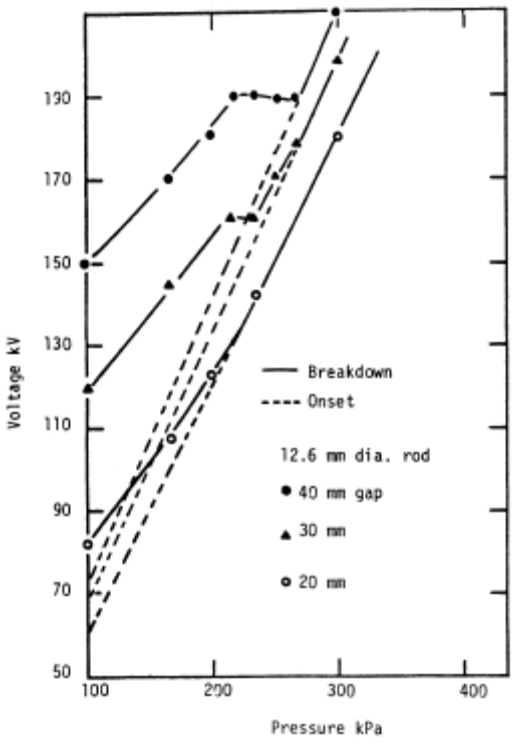

Fig.9 Effect of the gap length on the breakdown voltage-pressure characteristics of rod-plane SF_6 gap [25]

15 mm is the largest rod-plane gap in SF_6 breakdown experiments at 30 kHz. It is highly possible the breakdown voltage is so close to the onset voltage that no corona discharge can be observed.

Comparison with published experimental data

For the uniform field gaps, the breakdown voltage of SF_6 at 30 kHz linearly increases with pressure, as shown in Fig.10. The breakdown voltage for the 5 mm plane-plane SF_6 gap is approximately as twice as that of the 2.5 mm gap. It can be noted from Fig.11 that the 50 Hz Paschen curve for SF_6 matches the observed breakdown voltages in uniform field gaps at 30 kHz. This suggests that there is no significant difference in the

breakdown strength of SF_6 in uniform electric field between VLF/LF and power frequency.

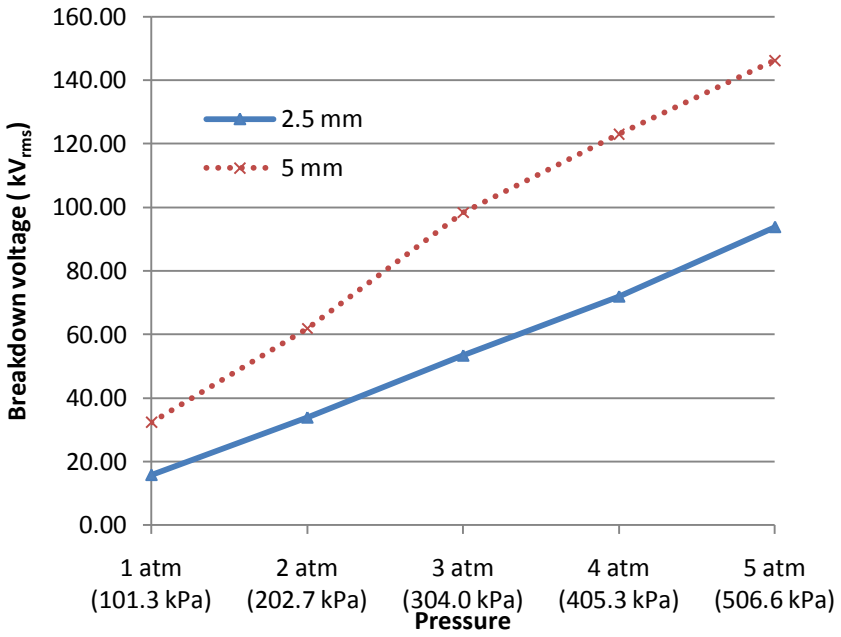

Fig.10 Breakdown voltage-pressure characteristic of plane-plane SF_6 gaps at 30 kHz

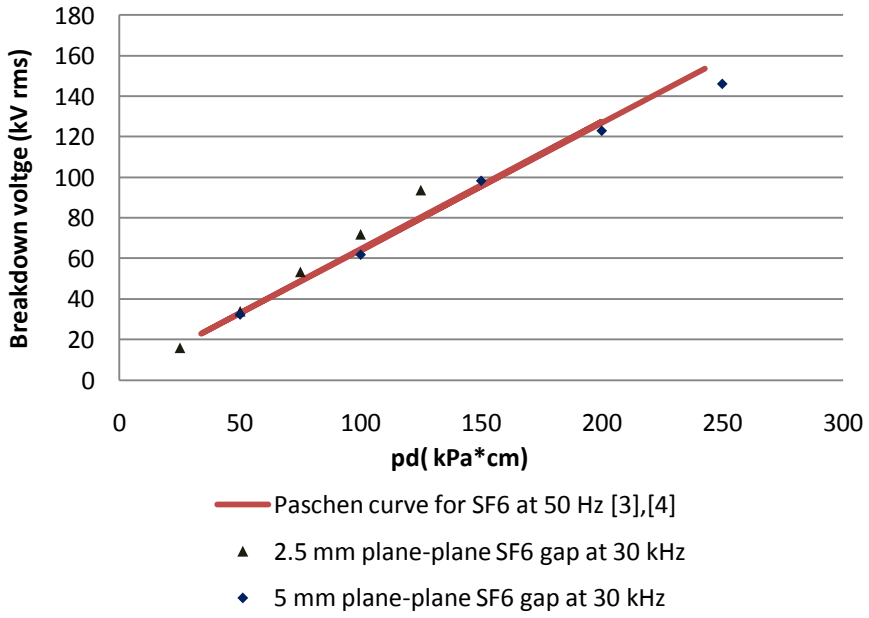

Fig.11 Paschen curve for SF_6 at 50 Hz and data at 30 kHz

However, the linearity between breakdown voltage and pressure was not observed from the non-uniform field rod-plane SF_6 gaps. As shown in Fig.12, the breakdown voltage is proportional to pressure, but the slope reduces in the pressure range from 2 atm to 4 atm. The reduction in slope occurs for both 8 mm and 15 mm rod-plane gaps. Nonlinearity of the breakdown voltage-pressure characteristic of SF_6 has also been reported for non-uniform DC electric fields with both positive and negative polarities [25]. A possible reason of nonlinearity has been attributed to the spark path changing from straight line to a curve, mention in reference [25].

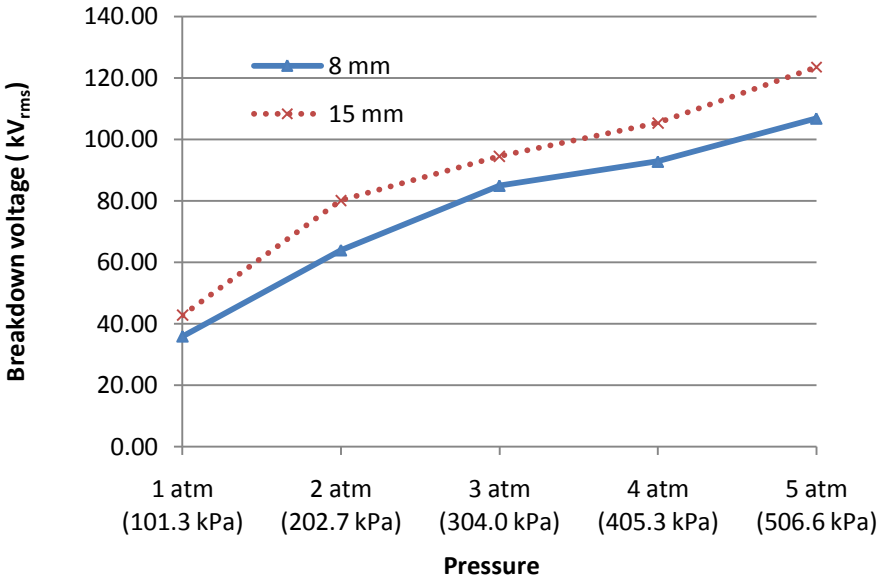

Fig.12 Breakdown voltage-pressure characteristic of rod-plane SF_6 gaps at 30 kHz

To better understand the dielectric properties of SF_6 in non-uniform electric fields at 30 kHz, a direct comparison with published data for power frequency is desired. However, breakdown gap configurations vary from experiment to experiment, which makes comparison difficult. The rod electrode radius and gap length, two of the most important parameters determining breakdown voltage, have different combinations in

published experimental data. Calculating the ratio of the breakdown voltage of SF_6 at higher pressure to that of 1 atm in same gap and frequency is an effective way to standardize experimental results. Fig.13 compares the breakdown voltage ratios for 50/60 Hz [8], DC [25] and 30 kHz. In this comparison, the electrode configurations are identical. Unlike the uniform scenario discussed in Fig.11, the breakdown voltage of SF_6 in non-uniform electric field at 30 kHz varies significantly from data obtained at power frequency, as shown in Fig.13. Therefore, it is not accurate to estimate dielectric performance of SF_6 in non-uniform electric field based on data at power frequency.

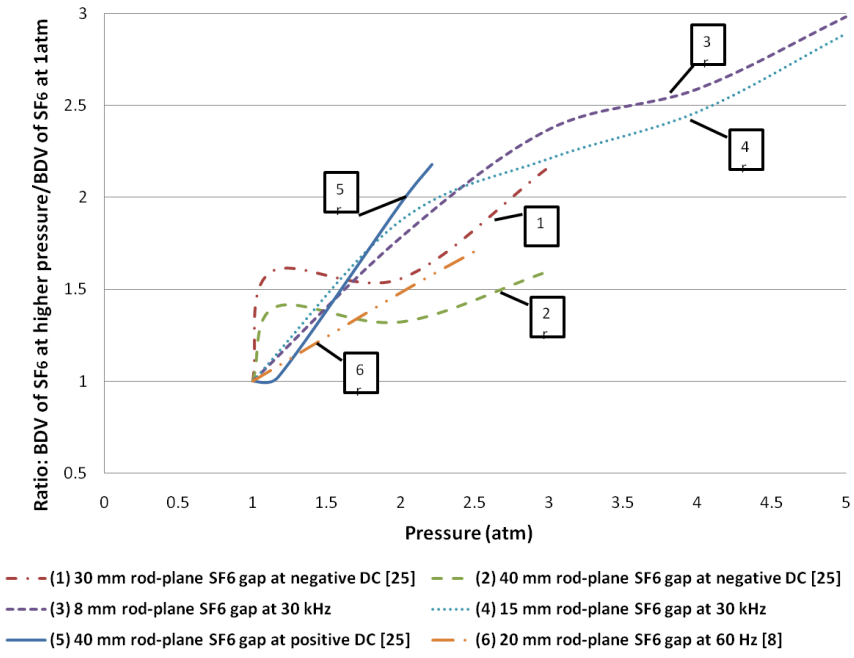

Fig.13. Ratio of the breakdown voltage of rod-plane SF_6 gap at high pressure to that at 1 atm, with the rod diameter of 13 mm

Breakdown experiments of air with 5mm plane-plane gap were conducted and experimental results are shown in Fig.14. In uniform field configuration, the breakdown voltage-pressure curves essentially overlap each other, indicating no significant

difference of observed breakdown voltage at 60 Hz or 30 kHz. However, for the non-uniform field configuration, the breakdown voltage in air at 30 kHz is somewhat reduced as shown in Fig.15. At higher pressures this difference increases. From Fig.13 and 14, it can be seen that the difference of breakdown voltages between 30 kHz and 60 Hz is more pronounced for SF_6 than air.

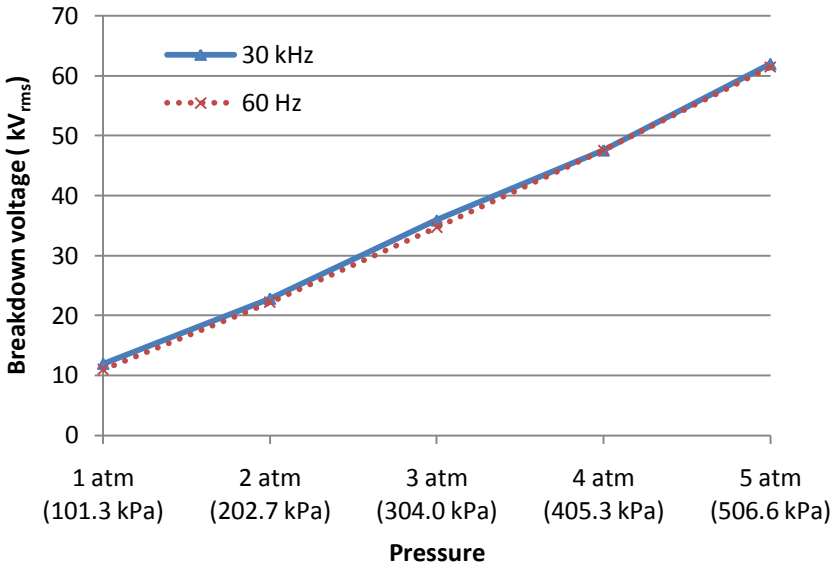

Fig.14 Breakdown voltage behavior of 5 mm plane-plane air gap at 30 kHz and 60 Hz

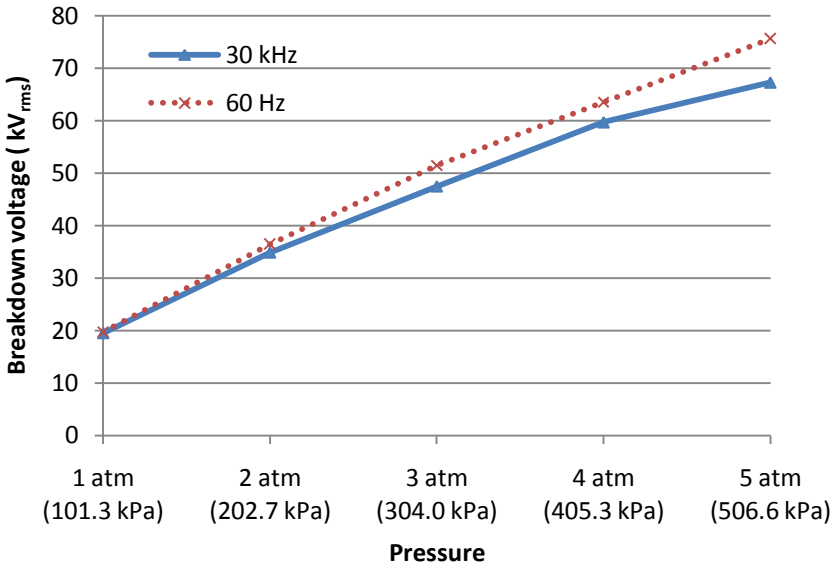

Fig.15 Breakdown voltage behavior of 15 mm rod-plane air gap at 30 kHz and 60 Hz

CHAPTER 4

ANALYSIS OF INFLUENCE OF GROUNDING METAL CHAMBER

Justification

All the breakdown experiments were conducted in the metal chamber. However, the bushings in practice are made of fibergrass tube surrounded by silicon rubber sheds as housing, and filled with compressed SF_6 [26]. It is necessary to take the influence of the grounded metal chamber into consideration, in order to make the investigation accurate and applicable.

Experimental Measurements

One plexiglass chamber is chosen as reference. The plexiglass chamber is shown in Fig.16. The experiments of air in the plexiglass chamber have been conducted by D. Rodriguez [27], [28]. Breakdown voltages in both chambers were compared. All experiments were conducted at ambient atmosphere with identical experimental conditions except the chamber configurations. 5 mm, 10 mm and 15 mm gaps were tested for plane-plane electrode configuration, and 8 mm, 15 mm and 45 mm gaps for rod-plane cases. The experimental data is listed in Table 8 and Table 9. Since those experiments tested ambient air breakdown voltage, the real breakdown was corrected by the temperature and ambient pressure correction factor. The last 10 breakdown voltages with deviation less than 5% were recorded for each test scenario and the average value was calculated. To compare the difference, the ratio of breakdown voltage in metal chamber to that in plexiglass chamber with same gap length is listed in Table 10. Five out of six groups of comparison are within 10% difference. The 15 mm rod-plane gap has the

greatest difference as 113.67%, and that for 5 mm plane-plane is 93.65%. These two gap scenarios were chosen to be simulated.

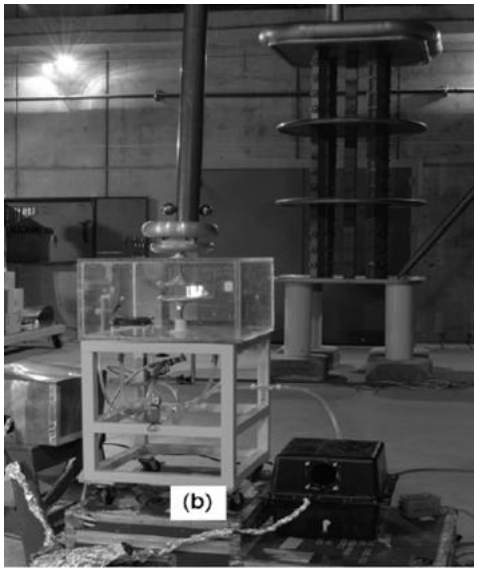

Fig.16 Plexiglass chamber [27]

Table 8

Breakdown voltage of plane-plane air gap at 1 atm in different chambers

Test #	Breakdown Voltage (kV rms)					
	5 mm gap		10 mm gap		15 mm gap	
	Metal	Plexiglass	Metal	Plexiglass	Metal	Plexiglass
1	11.13	11.66	20.46	21.77	30.13	30.62
2	10.80	11.65	20.36	21.71	30.14	30.36
3	11.02	11.79	20.55	21.66	29.84	30.45
4	10.88	11.82	20.84	21.67	30.29	30.54
5	11.04	11.78	21.01	21.66	30.33	30.34
6	10.99	11.69	20.92	21.72	30.47	30.30
7	10.93	11.77	20.36	21.63	30.53	30.54
8	10.97	11.68	20.40	21.71	29.20	30.46
9	11.07	11.69	21.10	21.73	30.54	30.57
10	10.97	11.70	20.90	21.79	30.47	30.56
AVE	10.98	11.72	20.69	21.71	30.19	30.48
STD	0.09	0.06	0.29	0.05	0.41	0.11
STD/AVE	0.86%	0.52%	1.40%	0.23%	1.36%	0.37%

Table 9

Breakdown voltage of rod-plane air gap at 1 atm in different chambers

Test #	Breakdown Voltage (kV rms)					
	8 mm gap		15 mm gap		45 mm gap	
	Metal	Plexiglass	Metal	Plexiglass	Metal	Plexiglass
1	16.38	15.91	19.70	17.30	28.06	27.13
2	15.71	15.55	19.83	17.29	28.11	27.10
3	16.58	15.21	18.60	17.31	29.14	27.74
4	16.49	15.23	19.93	17.97	26.92	28.78
5	16.87	15.39	19.41	17.32	28.65	29.29
6	17.08	15.92	19.91	18.12	29.28	28.03
7	15.78	15.14	20.37	16.64	28.52	26.28
8	15.64	15.22	20.12	17.32	28.14	28.01
9	16.48	15.90	19.73	16.63	28.13	29.27
10	16.88	15.18	19.63	17.62	28.98	27.75
AVE	16.39	15.46	19.72	17.35	28.39	27.94
STD	0.52	0.33	0.48	0.48	0.69	0.97
STD/AVE	3.15%	2.11%	2.41%	2.78%	2.43%	3.48%

Table 10

Ratio of breakdown voltage in the metal chamber to that in plexiglass chamber

Gap configuration	Gap length (mm)	Ratio
Plane-Plane	5	93.65%
	10	95.32%
	15	99.08%
Rod-Plane	8	105.99%
	15	113.67%
	45	101.62%

Simulation Results

In order to accurately analyze the influence of the grounding chamber on the breakdown voltage, the Coulomb 8.0 software package was used to simulate the electric field in the chamber. For each chamber, the plane-plane electrode configuration and the rod-plane electrode configuration were simulated respectively. Totally four models were

established. The model's geometry is identical to the actual dimension of the object. The main parts of the chamber were simulated in the model with necessary simplifications. Every part of the chamber in the model was assigned a corresponding material with its conductivity and permittivity. Since boundary element method is applied in Coulomb software, triangular boundary elements were distributed on the surface of the model. Over 8000 elements were assigned for every model which ensured the accuracy of the simulation with a tolerance of less than 8%.

The electric field distribution, especially the maximum electric field value, was focused in the whole simulation analysis, as the maximum electric field value determines the breakdown voltage. To clearly analyze the model and to make comparison visual, four plots are displayed for every model, named as model plot, voltage plot, E-field plot and validation plot.

1) The model plot presents the 3D model with triangular boundary elements in Coulomb. The geometric difference is clearly noticed in model plot.
2) The voltage plot demonstrates the voltage distribution along the axis of the gap.
3) The E-field plot is the focus of simulation analysis, showing the electric field distribution along the axis of the gap.
4) The validation plot shows the integration of tangent component of electric field strength. The high value consistency between the integration value of electric field and voltage value originally applied on the gap indicates the accuracy of simulation.

Plane-plane gap

The gap length was set as 5 mm gap since that was the maximum gap for uniform electric field gaseous breakdown experiment, as well as that was the gap where the greatest deviation occurs in experimental results for different chamber. The applied voltage was chosen as 10 kV for both plane-plane models according to the experimental breakdown voltage. The model analysis plots for plane-plane gap are shown from Fig.17 to Fig.24.

The maximum voltage drop is in the air gap between the two electrodes. The electric field strength keeps constant for both models, matching the feature of uniform electric field breakdown. The deviations seen from validation plots for both plane-plane gaps are within tolerance, less than 10%.

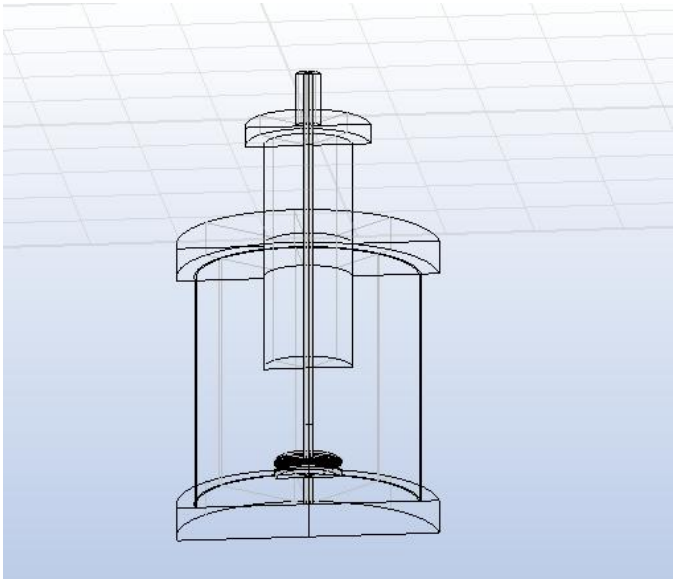

Fig.17 Model plot for plane-plane gap in metal chamber

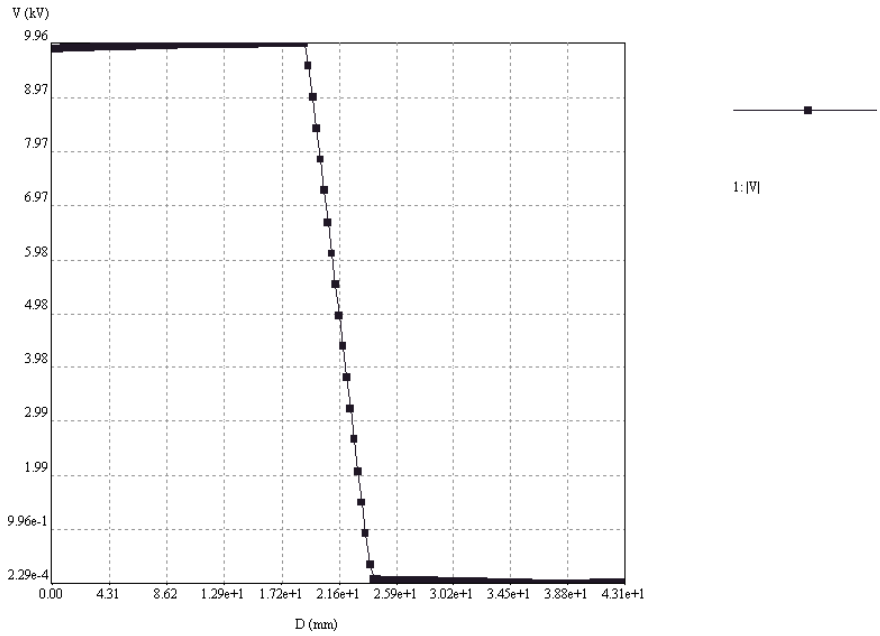

Fig.18. Voltage plot for plane-plane gap in metal chamber

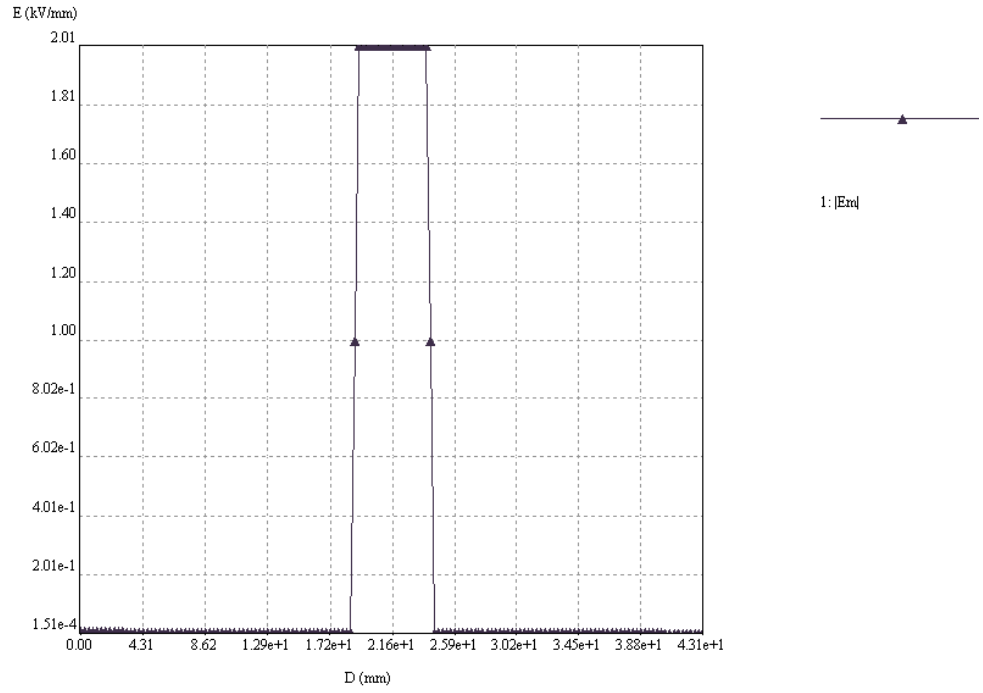

Fig.19. E-field plot for plane-plane gap in metal chamber

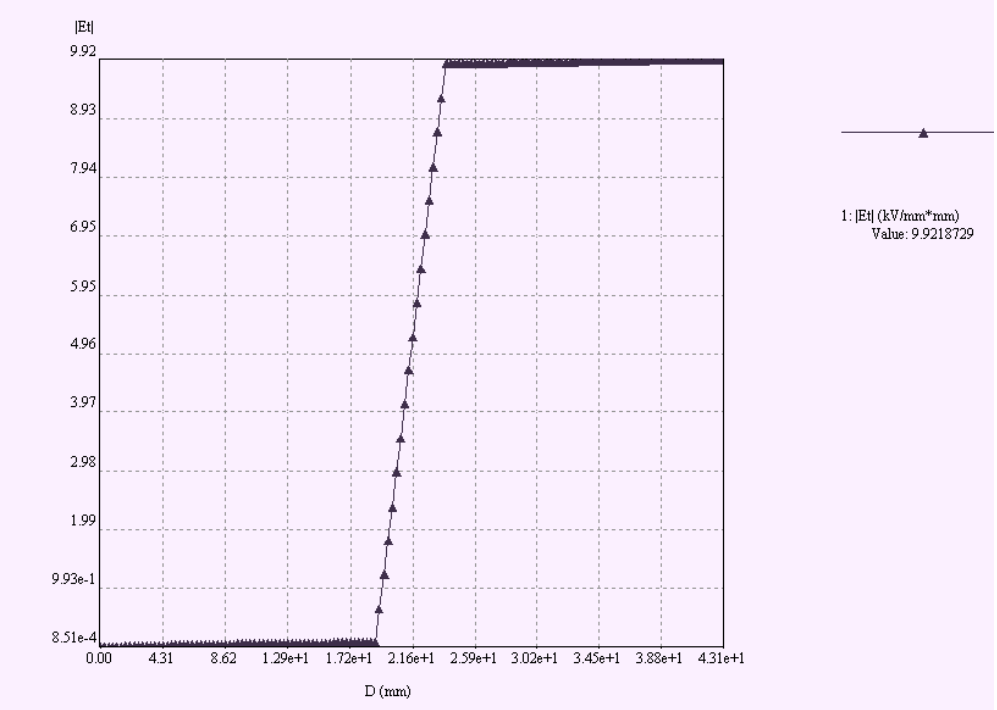

Fig.20. Validation plot for plane-plane gap in metal chamber

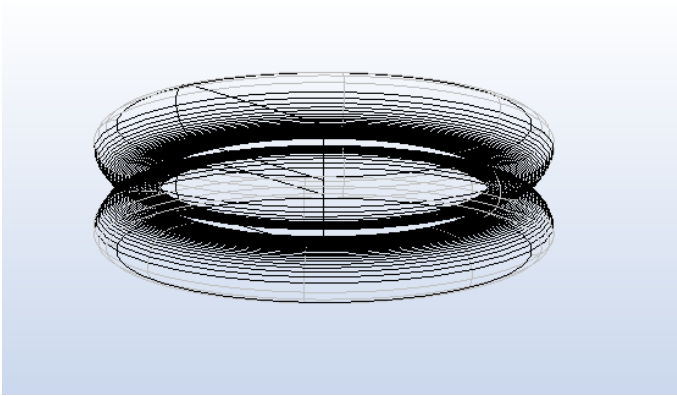

Fig.21. Model plot for plane-plane gap in plexiglass chamber

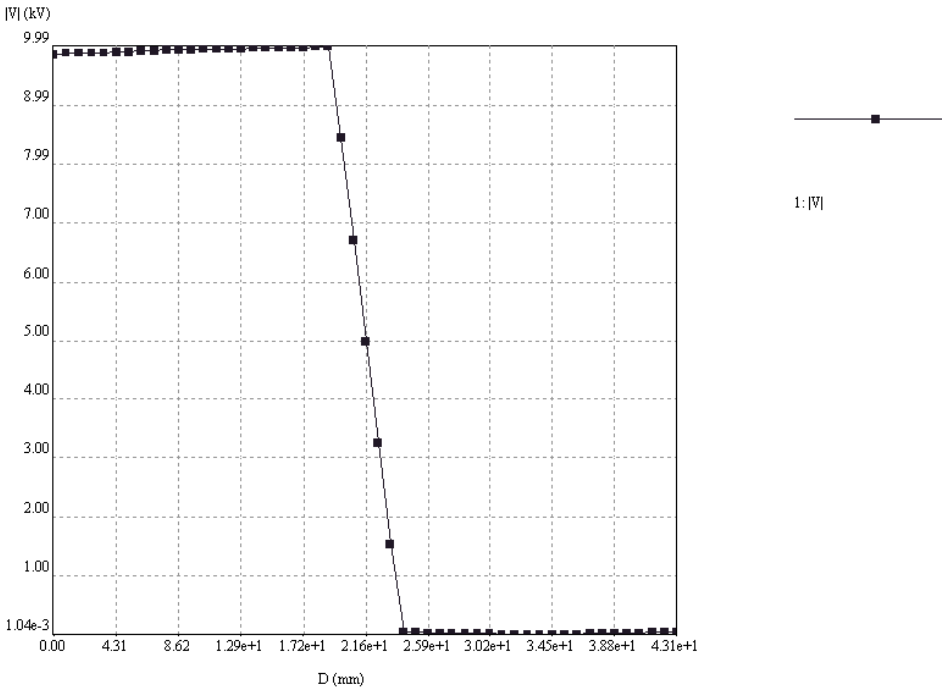

Fig.22 Voltage plot for plane-plane gap in plexiglass chamber

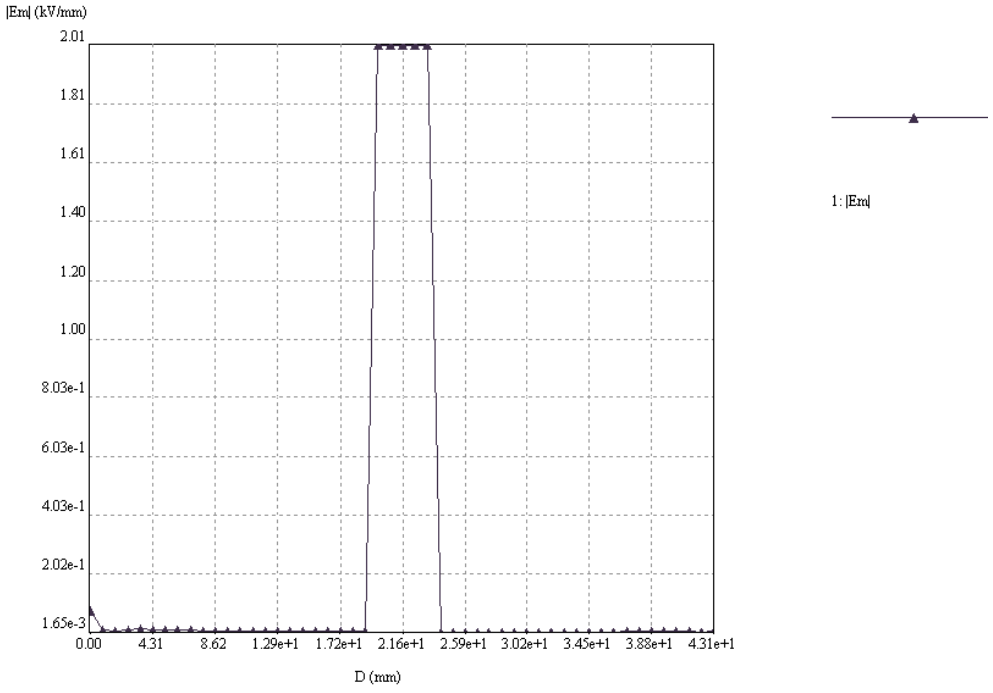

Fig.23 E-field plot for plane-plane gap in plexiglass chamber

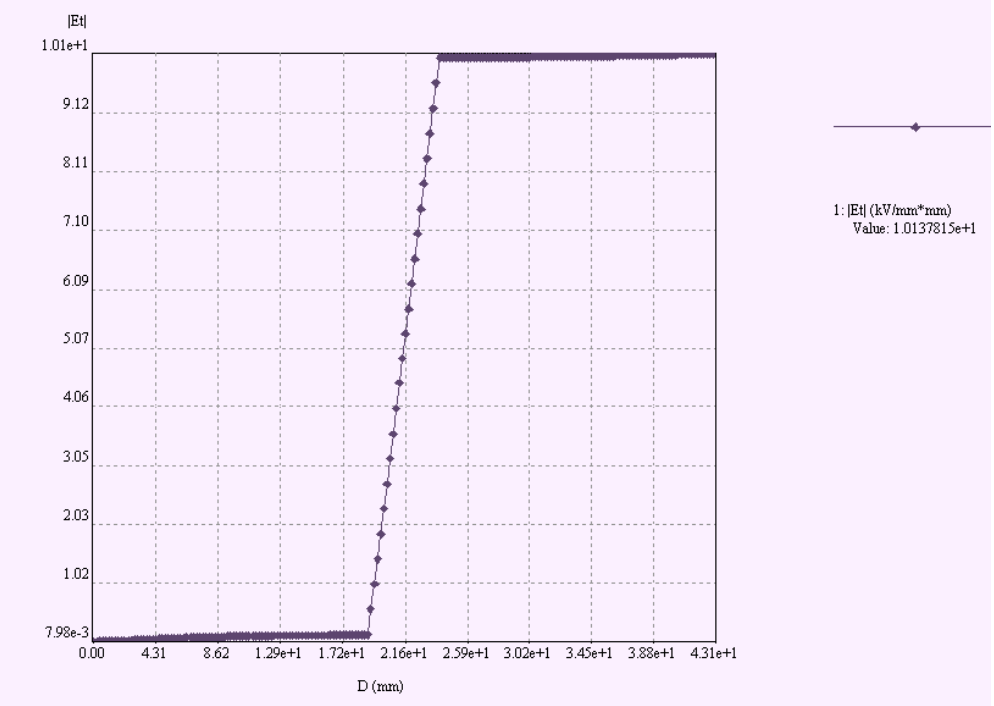

Fig.24 Validation plot for plane-plane gap in plexiglass chamber

Rod-plane gap

In the models, the gap length was set as 15 mm and the applied voltage was 20 kV. The model analysis plots for rod-plane gap are shown from Fig.25 to Fig.32.

The maximum voltage also drops in the air gap. However, the electric field distribution changes dramatically. There is a pulse observed in the E-field graph in between electrodes. The maximum electric field strength occurs at the tip of the rod electrode. The deviations seen from validation plots for both rod-plane gaps are within tolerance, less than 10%.

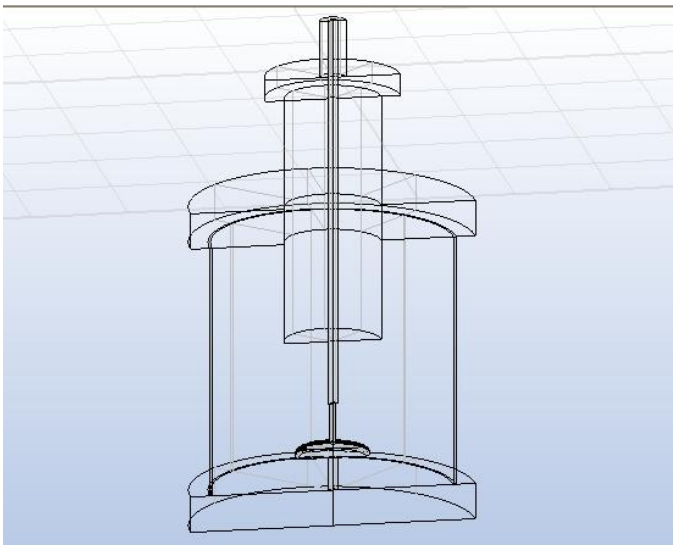

Fig.25 Model plot for rod-plane gap in metal chamber

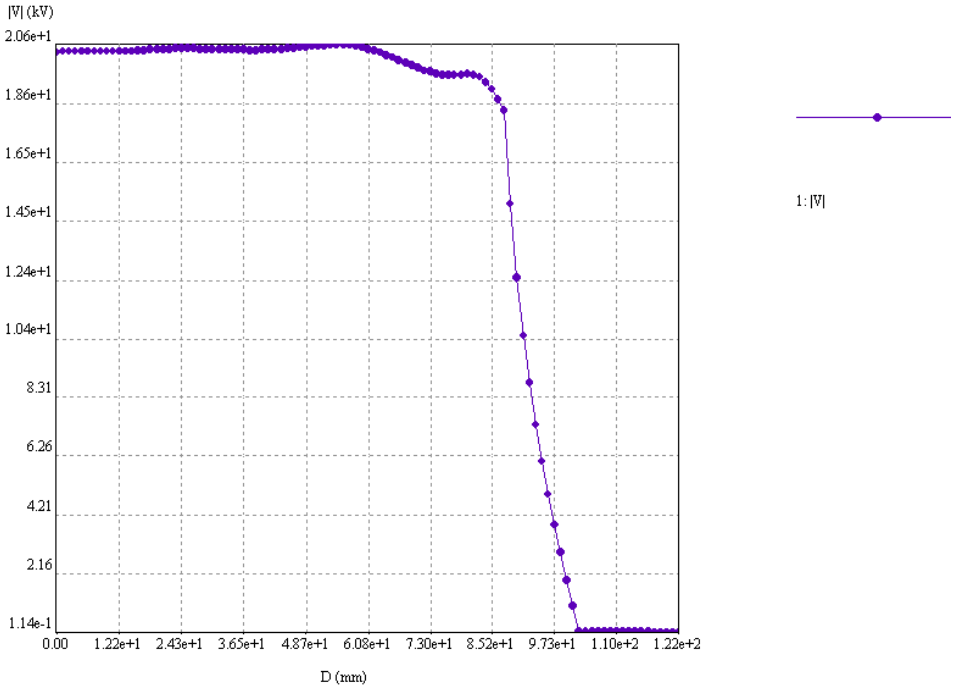

Fig.26 Voltage plot for rod-plane gap in metal chamber

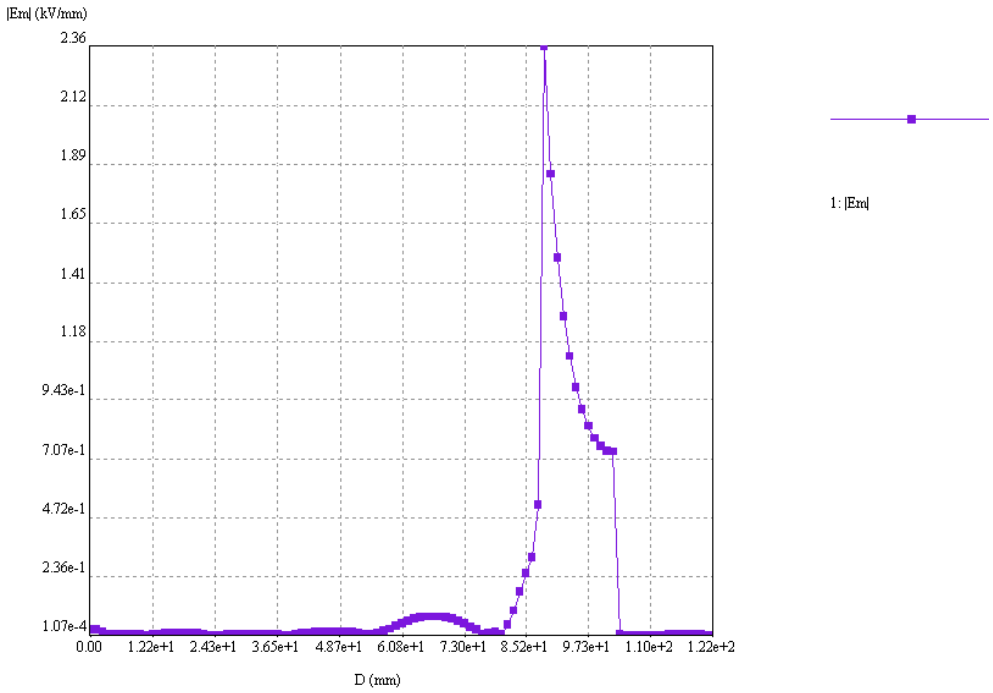

Fig.27 E-field plot for rod-plane gap in metal chamber

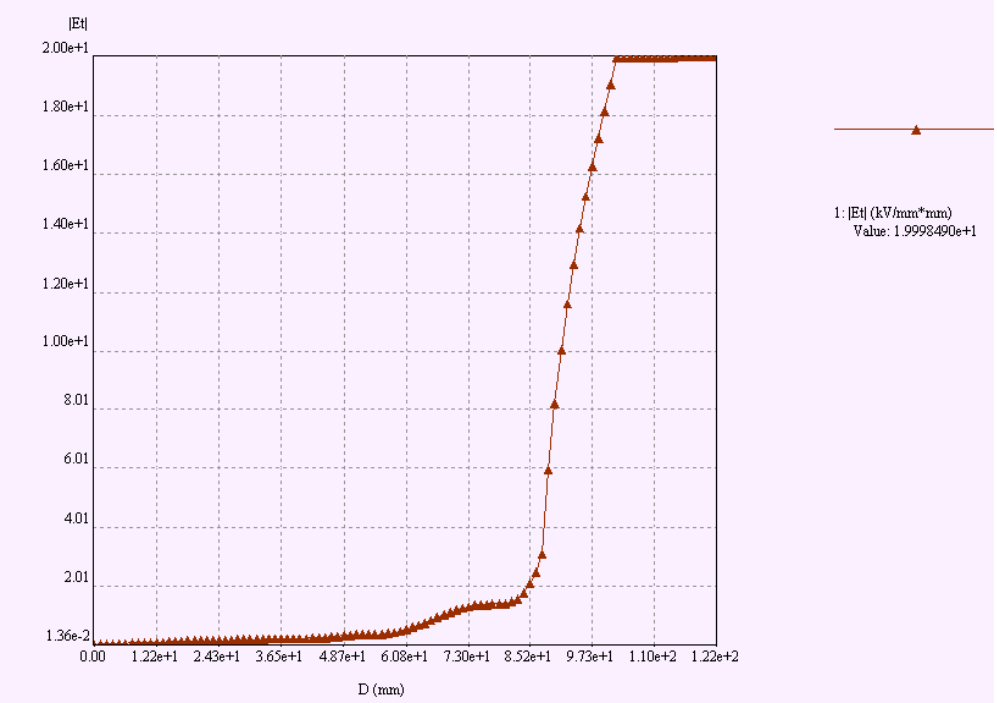

Fig.28 Validation plot for rod-plane gap in metal chamber

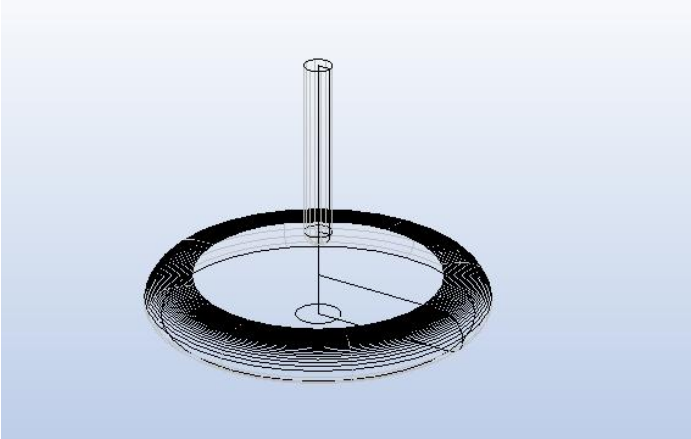

Fig.29 Model plot for rod-plane gap in plexiglass chamber

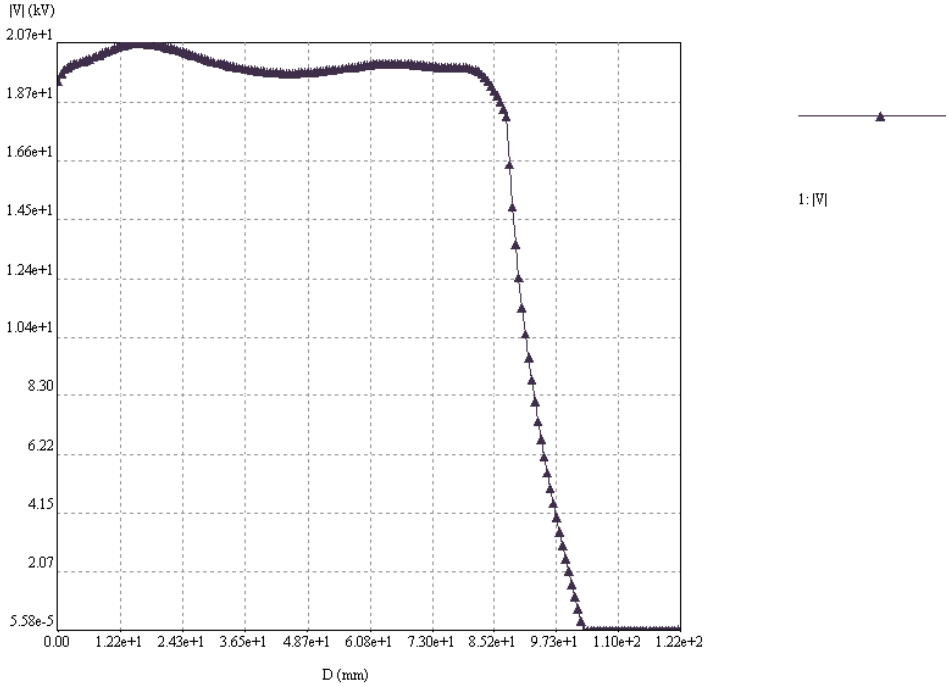

Fig.30 Voltage plot for rod-plane gap in plexiglass chamber

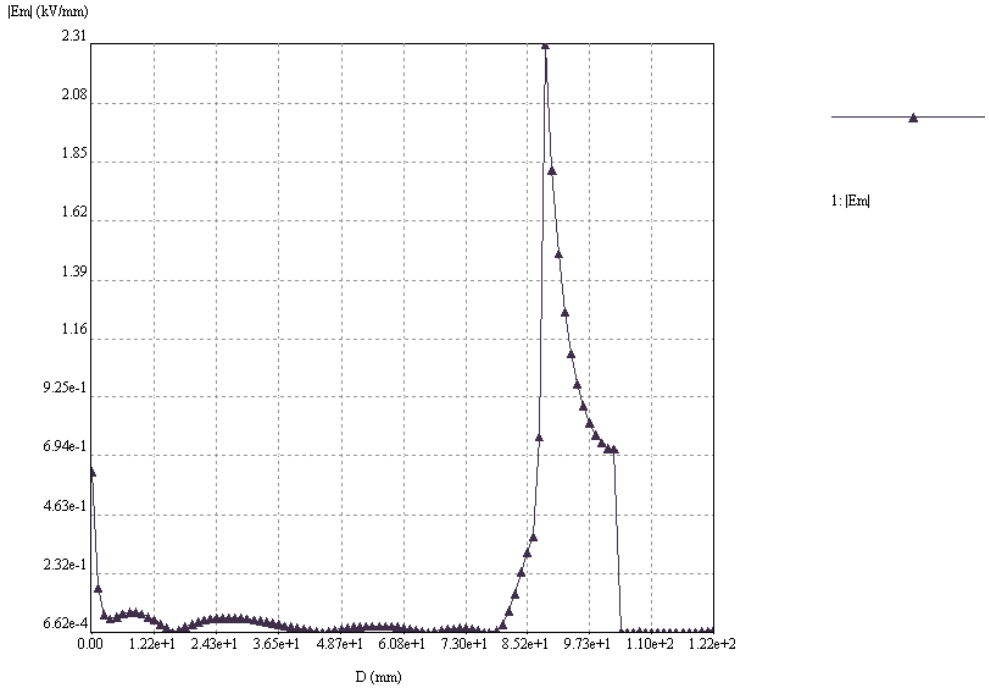

Fig.31 E-field plot for rod-plane gap in plexiglass chamber

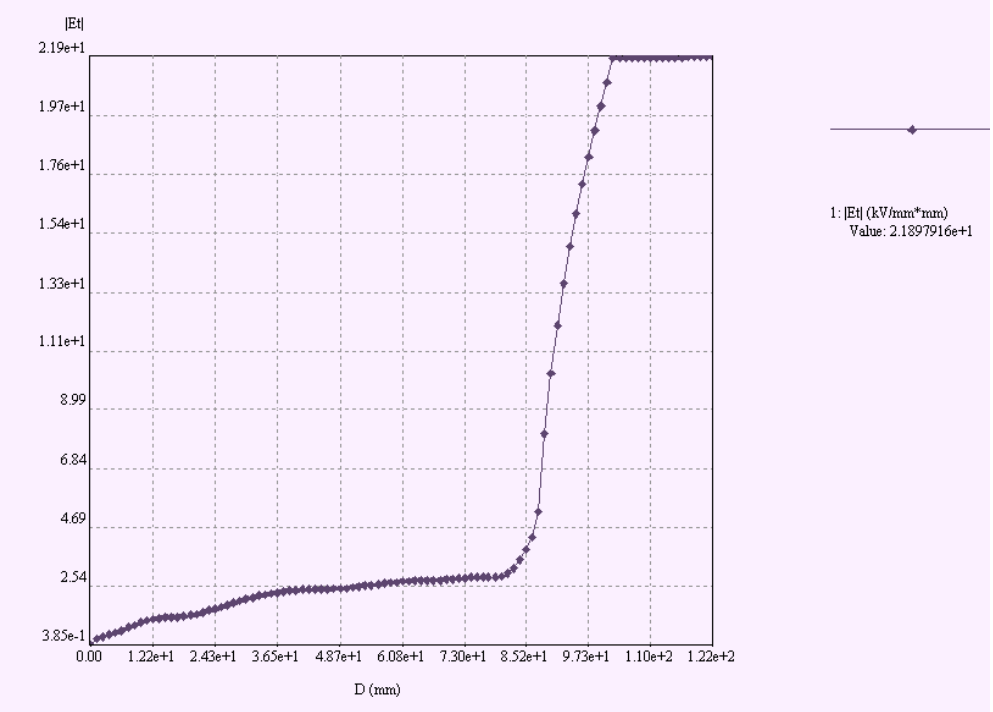

Fig.32 Validation plot for rod-plane gap in plexiglass chamber

Table 11

Summary of simulation results

Parameter	5 mm plane-plane gap		15 mm rod-plane	
	Metal chamber	Plexiglass chamber	Metal chamber	Plexiglass chamber
Applied voltage (kV)	10	10	20	20
Voltage plot (kV)	9.96	9.99	20.6	20.7
E-plot (kV/mm)	2.01	2.01	2.36	2.31
Validation plot (kV)	9.92	10.1	20	21.9
Tolerance (%)	0.4%	1.1%	2.9%	5.8%

Discussion

The simulation results match with the experimental data. The difference in experimental data is relatively bigger than simulation, because the noise cannot be eliminated in the process of laboratory experiments. The maximum electric field value of air gap agrees with the data in previous literature, about 3 kV/mm of peak value.

The metal grounding influence is more obvious in non-uniform electric field distribution than that in uniform electric field distribution, but both are in tolerance. Considering the dimension of the metal chamber in our experiment is big enough when compared with the dimension of electrodes, the electric field distribution in the gap is slightly influenced by the surrounding metal.

CHAPTER 5

DATA ANALYSIS

Objective

It is useful for bushing design and optimization to provide empirical models for estimating dielectric performance of SF_6. In this study, the pressure correction factor is defined as the ratio of the breakdown voltage at 30 kHz for various pressures to that of air at 60 Hz for 1 atm with the same gap configuration. This parameter takes advantage of ample amount of available data of air at power frequency to estimate the dielectric performance at VLF/LF. In the following, regression analysis is used to establish models for pressure correction factors.

Dielectric Property Study of SF_6 at VLF/LF

The regression analysis for SF_6 plane-plane and rod-plane gaps at 30 kHz is shown in Fig.33 and Fig.37 respectively. In order to meet normality and constant variance, transformation of response or regressor is necessary. Through various trials of transformation, models presented in the paper best balance these two requirements. The parameter 'Cp' stands for the pressure correction factor. R^2 and adjusted R^2 give information about the goodness of fit of a model. R^2, coefficient of determination, indicates the proportion of variability in a data set explained by the statistical model. R^2 can be inflated by adding more terms to the model, even they are insignificant. Adjusted R2 will decrease when insignificant terms are added in the model as a penalty. Checking both R^2 and adjusted R^2 provides more accurate view on how well a model is expected to predict new values. Normally, R^2 and adjusted R^2 are in range of 0 to1, closer to1 with

improvement of fitness. Models with these values in excess of 90% are considered accurate. The level of significance, or critical p-value, used for the models is 0.05. Models with p-values of 0.05 or lower are considered statistically significant with very low probability of failure. Fig.34 and Fig.38 demonstrates how well these regression models fit the experimental data. Note that the deviation of data from the fitted line in Fig.34 at 5 atm is bigger than other pressures. One possible reason is that the influence of gap length enhance at higher pressure, since the two clusters of data belong to two gap lengths (2.5 mm and 5 mm). In addition, breakdown experiments may bring in more natural noise at higher applied voltage, corresponding with higher pressure. However, the deviation is not severe enough to violate constant variance requirement. Normality checks for plane-plane and rod-plane models are demonstrated Fig. 35 and Fig.39 respectively. Fig.36 and Fig.40 show constant variance checks.

Regression Analysis: Cp versus Pressure

The regression equation is
log10(Cp) = 0.4512 + 1.028 log10(Pressure)

S = 0.0244903 R-Sq = 99.1% R-Sq(adj) = 99.1%

Analysis of Variance

Source	DF	SS	MS	F	P
Regression	1	3.22050	3.22050	5369.53	0.000
Error	48	0.02879	0.00060		
Total	49	3.24929			

Fig.33 Regression analysis of pressure correction factor for plane-plane SF_6 gap

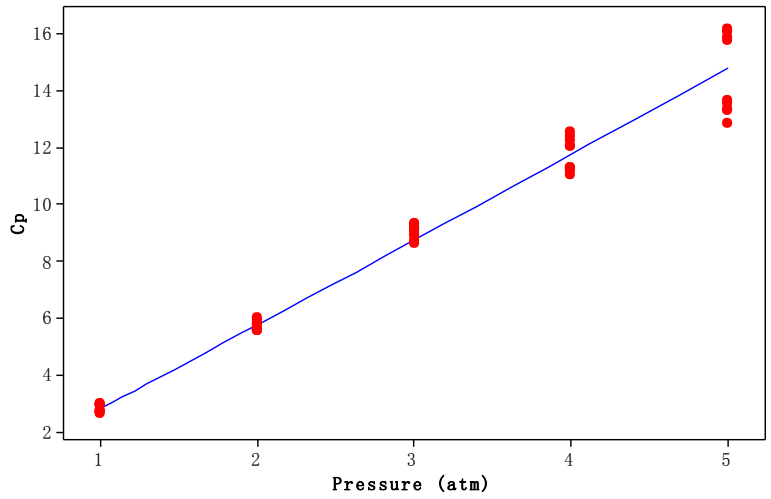

Fig.34 Fitted line plot for the pressure correction factor model of plane-plane SF_6 gap

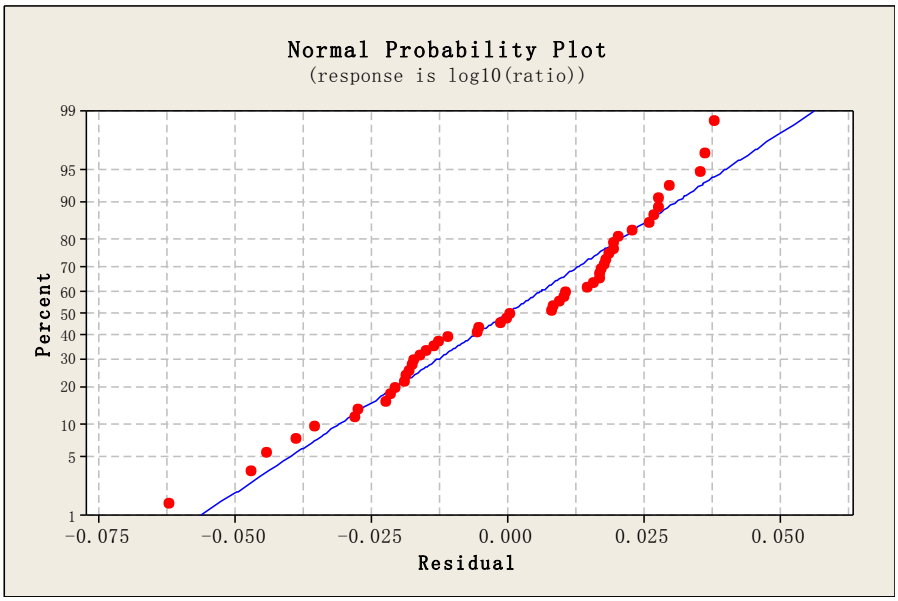

Fig. 35 Normality check for the pressure correction factor model of plane-plane SF_6 gap

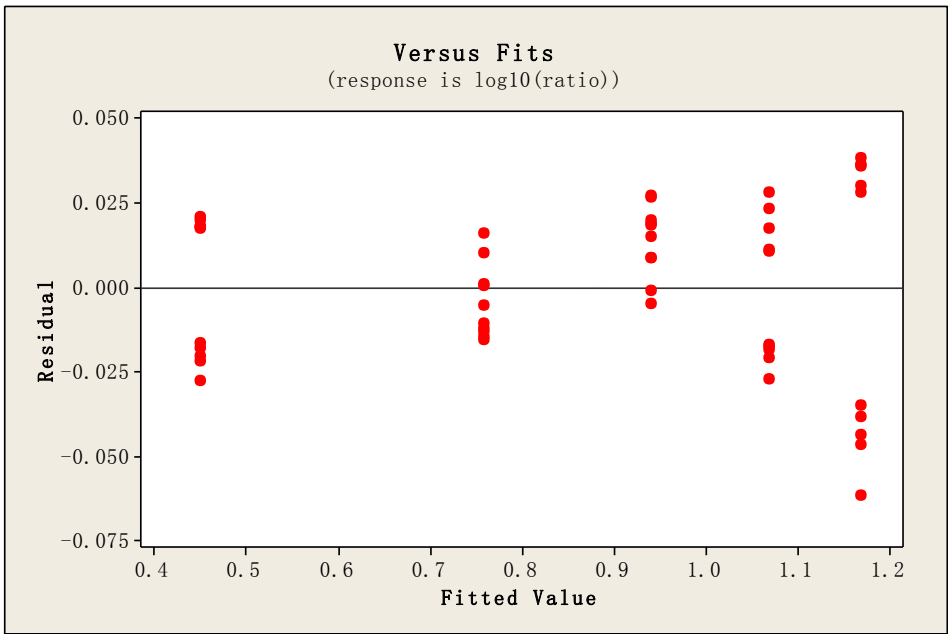

Fig.36 Constant variance check for the pressure correction factor model of plane-plane SF_6 gap

Regression Analysis: Cp versus Pressure

The regression equation is
Cp = 2.180 + 5.834 log10(Pressure)

S = 0.245134 R-Sq = 97.3% R-Sq(adj) = 97.2%

Analysis of Variance

Source	DF	SS	MS	F	P
Regression	1	103.705	103.705	1725.81	0.000
Error	48	2.884	0.060		
Total	49	106.590			

Fig.37 Regression analysis of pressure correction factor for rod-plane SF_6 gap

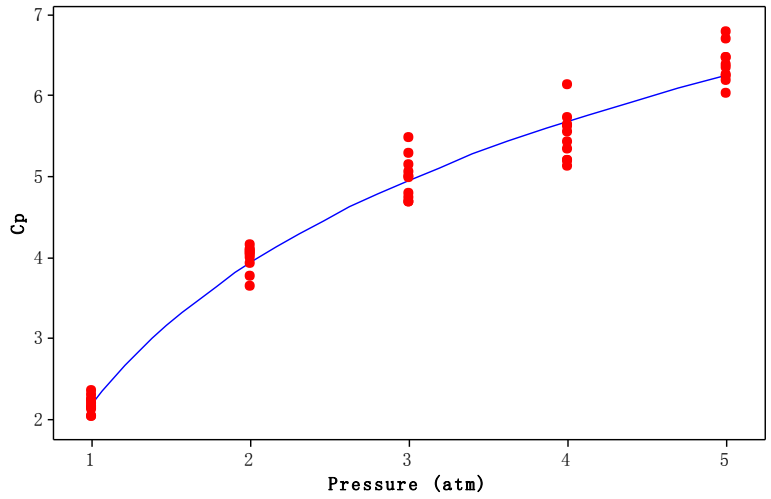

Fig.38 Fitted line plot for the pressure correction factor model of rod-plane SF_6 gap

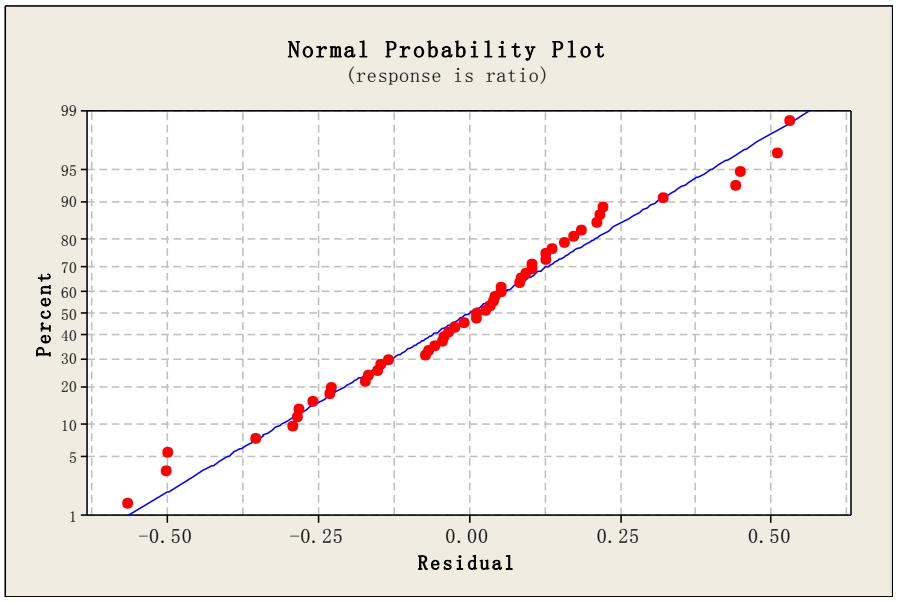

Fig.39 Normality check for the pressure correction factor model of rod-plane SF_6 gap

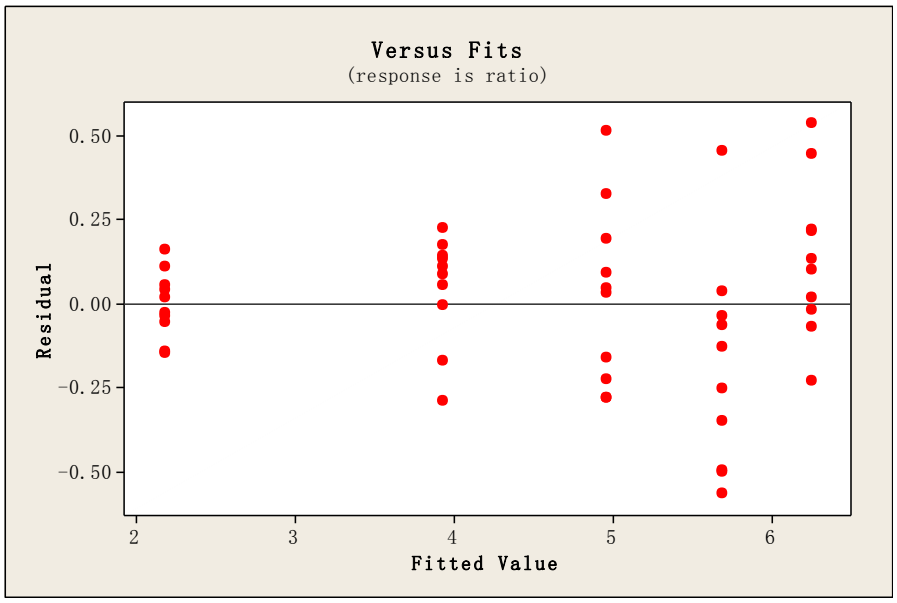

Fig.40 Constant variance check for the pressure correction factor model of rod-plane SF_6 gap

Dielectric Property Study of Air at VLF/LF

To quantitatively compare the breakdown voltages of SF_6 and air at VLF/LF, regression analysis for data of air at 30 kHz is desirable. Similarly, the pressure correction factors of air are presented in Fig.41 and Fig.43. For ratio in this case, the numerator is the breakdown voltage of air at various pressures at 30 kHz instead of SF_6. The denominator is still the breakdown voltage of air at 60 Hz at 1atm. According to Fig.42 and Fig.44, both models fit the data well.

Regression Analysis: Cp versus Pressure

The regression equation is
Cp = - 0.1280 + 1.137 Pressure

S = 0.121857 R-Sq = 99.5% R-Sq(adj) = 99.5%

Analysis of Variance

Source	DF	SS	MS	F	P
Regression	1	64.6606	64.6606	4354.53	0.000
Error	23	0.3415	0.0148		
Total	24	65.0021			

Fig.41 Regression analysis of pressure correction factor for plane-plane air gap

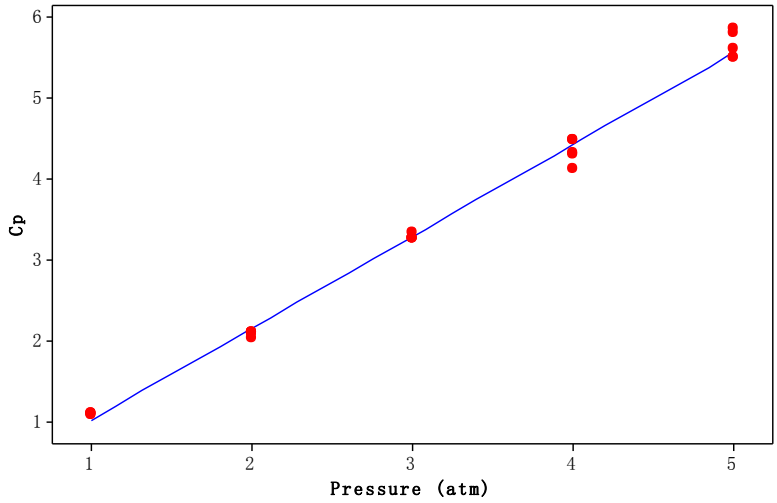

Fig.42 Fitted line plot for pressure correction factor for plane-plane air gap model

Regression Analysis: Cp versus Pressure

The regression equation is
Cp = 0.4873 + 0.6111 Pressure

S = 0.118384 R-Sq = 98.3% R-Sq(adj) = 98.2%

Analysis of Variance

Source	DF	SS	MS	F	P
Regression	1	18.6706	18.6706	1332.22	0.000
Error	23	0.3223	0.0140		
Total	24	18.9930			

Fig.43 Regression analysis of pressure correction factor for rod-plane air gap

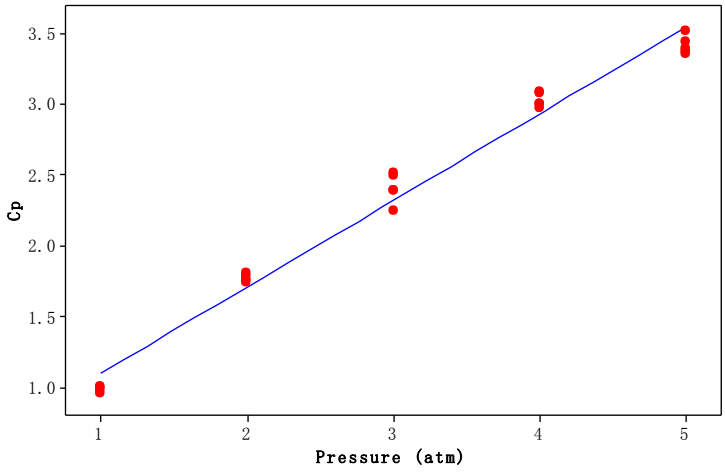

Fig.44 Fitted line plot for pressure correction factor for rod-plane air gap model

Table 12 lists the regression models of pressure correction factors for SF_6 and air at 30 kHz. All coefficients keep 2 decimals due to precision of experimental data. The comparison of breakdown voltage between SF_6 and air is valuable information for bushing design. In previous studies, the ratio of breakdown voltage of SF_6 to that of air for the same gap length and pressure is commonly calculated as reference of comparison. Different researchers presented various values from 1.5 to 2.7 under different

experimental conditions [29], [30] .All of the values are at power frequency. The ratio at VLF/LF has not been calculated so far.

Table 12

Summary of regression models

Gas type	Gap configuration	Regression model for pressure correction factor
SF_6 at 30 kHz	Plane-plane	$k_p = 2.83p^{1.03}$
	Rod-plane	$k_p = 2.18 + 5.83 \log_{10} p$
Air at 30 kHz	Plane-plane	$k_p = -0.13 + 1.14p$
	Rod-plane	$k_p = 0.49 + 0.61p$

Taking advantage of regression models for SF_6 and air at 30 kHz, the ratio can be easily calculated in the whole range of pressure from 1 to 5 atm. Fig.45 shows the ratio of breakdown voltage of SF_6 at 30 kHz to that of air in both uniform and non-uniform electric fields.

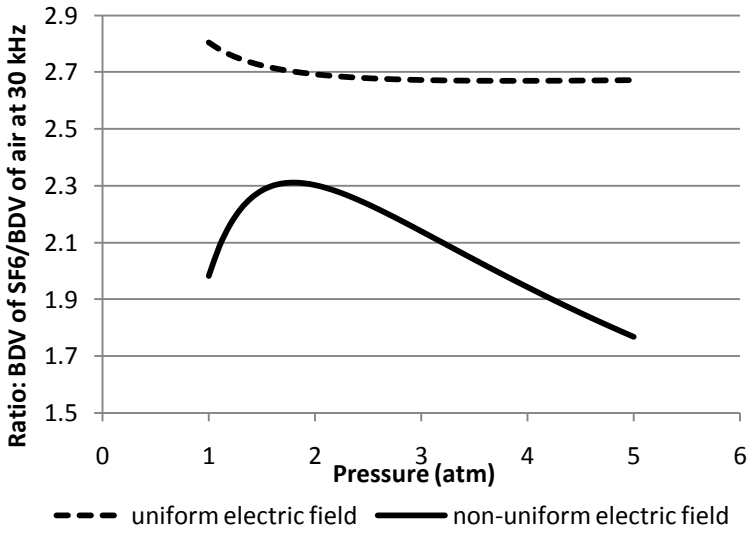

Fig.45 Dielectric strength of SF_6 at 30 kHz relative to air

These plots have been generated from regression models proposed in Table 12. The breakdown voltage of SF_6 at 30 kHz is almost constant as 2.7 times as that of air in uniform electric field. For non-uniform configuration this ratio changes with pressure.

CHAPTER 6

CONCLUSION AND FUTURE WORK

This paper focuses on the breakdown voltage of compressed SF_6 at VLF/LF. Measurements of the breakdown strength of SF_6 and air have been carried out for both uniform and non-uniform gaps over a range of pressures from 1-5 atm. The shape of the breakdown voltage-pressure curve of SF_6 in a uniform electric field at 30 kHz is similar to that at 60 Hz. However, when the field is non-uniform a significant difference occurs in the shape of the breakdown voltage-pressure curve of SF_6 versus that for air. Regression models for the breakdown strength versus pressure have been built from on the measured data. These models can be used to estimate the breakdown strength of compressed SF_6 at VLF/LF, given data of air at 60 Hz with same gap length. In addition, these models can compare the breakdown strength of SF_6 and air at VLF/LF. It is shown that SF_6 in a uniform field has breakdown strength of 2.7 times that of air over the entire pressure range investigated in VLF/LF. For the non-uniform field case, the ratio of the breakdown strength of SF_6 to that of air is less and varies with pressure, having a maximum of 2.3 at a pressure of 1.8 atm. This corresponds with the slope shift in the breakdown voltage-pressure characteristic of rod-plane SF_6 gap. This could be due to the fact that the non-uniform electric field impacts the ionization and attachment coefficients of SF_6 and air to various degrees. This aspect needs further study. The empirical models presented provide an effective way to use the existing data for breakdown of air at 60 Hz to evaluate the dielectric performance of SF_6 for the design of VLF/LF high voltage equipment. One area for future investigation is cylindrical gaps. In that case the field is non-uniform, varying as 1/r, but not nearly as much as in the rod-plane configuration.

Given that the rod-plane configuration with SF_6 has a breakdown characteristic significantly different than that for uniform fields it is likely that the variation for cylindrical gaps will be different as well. This is an important configuration for the design of VLF/LF high voltage hardware such as feed-through bushings and coaxial cables and needs to be investigated further.

REFERENCES

[1] P. M. Hansen, A. D. Watt. "VLF/LF High-Voltage Design and Testing." Technical Report 1904, SPAWAR, San Diego, CA, 2003. Print.

[2] Menju S, Takahashi K. "DC Dielectric Strength of a SF_6 Gas Insulated System." *IEEE Transactions on Power Apparatus and Systems* 97 (1978): 217-224. Web.

[3] Malik NH, Qureshi AH. "Breakdown Mechanisms in Sulphur-Hexafluoride." *IEEE Transactions on Electrical Insulation* 13 (1978): 135-145. Web.

[4] Kawaguchi Y, Sakata K, Menju S. "Dielectriic Breakdown of Sulphur Hexafluoride in Nearly Uniform Fields." *IEEE Transactions on Power Apparatus and Systems* 3 (1971): 1072-1078. Web.

[5] Berg Daniel, Works CN. "Effect of Space Charge on Electric Breakdown of Sulfur Hexafluoride in Non-uniform Fields." *Transactions of the American Institute of Electrical Engineers* 77 (1958): 820-823. Web.

[6] Takuma T. "Discharge Characteristics of Gaseous Dielectrics." *IEEE Transactions on Electrical Insulation* 6 (1986): 855- 867. Web.

[7] Camilli G, Chapman JJ. "Gaseous Insulation for High-Voltage Apparatus." *Transactions of the American Institute of Electrical Engineers* 1 (1947): 1463-1470. Web.

[8] Azer AA, Comsa RP. "Influence of Field Nonuniformity on the Breakdown Characteristics of Suliur Hexafluoride." *IEEE Transactions on Electrical Insulation* 4 (1973): 136-142. Web.

[9] Raju GG. *Gaseous Electronics Theory and Practice*. Taylor & Francis, 2006. Print.

[10] Zwicky M. "Breakdown Phenomena in SF_6 and Very Inhomogeneous Large Rod-Plane Gaps under 50 HZ-AC and Positive Impulse Voltages." *IEEE Transactions on Electrical Insulation* 3 (1987): 317-324. Web.

[11] Bins DF, Hood RJ. "Breakdown in sulphur hexafluoride and nitrogen under direct and impulse voltages." *Proceedings of the Institution of Electrical Engineers* 16 (1969): 1962-1968. Web.

[12] Anis H, Srivastava K.D. "Breakdown of Rod-Plane Gaps in SF_6 under Positive Switching Impulses." *IEEE Transactions on Power Apparatus and Systems* 101 (1982): 537-546. Web.

[13] Fatehchand RRT. "The electrical breakdown of gaseous dielectrics at high frequencies." *Proceedings of the IEE-Part C* 104 (1957): 489-495. Web.

[14] Tetenbaum SJ, MacDonald AD, Bandel HW. "Microwave Breakdown of SF_6." *IEEE Transactions on Plasma Science* 1 (1973): 55-57. Web.

[15] Maconald AD. *Microwave Breakdown in Gases.* New York: John Wiley and Sons, Inc., 1966. Print.

[16] Cookson Alan H, Wootton Roy E. "AC Corona and Breakdown Characteristics for Rod Gaps in Compressed Hydrogen, SF_6 AND Hydrogen-SF_6 Mixtures." *IEEE Transactions on Power Apparatus and Systems* 2 (1978): 415-423. Web.

[17] Malik NH, Qureshi AH. "A Review of Electrical Breakdown in Mixtures of SF_6 and Other Gases." *IEEE Transactions on Electrical Insulation* 1 (1979): 1-13. Web.

[18] Malik NH, Qureshi AH, Theophilus GD. "Static Field Breakdown of SF_6-N2 Mixtures in Rod-Plane Gaps." *IEEE Transactions on Electrical Insulation* 2 (1979): 61- 69. Web.

[19] Okabe S, Yuasa S, Kaneko S. "Evaluation of Breakdown Characteristics of Gas Insulated Switchgears for Non-standard Lightning Impulse Waveforms - Breakdown Characteristics for Non-standard Lightning Impulse Waveforms Associated with Lightning Surges." *IEEE Trans. Dielectr. Electr. Insul* 2 (2008): 407-415. Web.

[20] Okabe S, Yuasa S, Kaneko S. "Evaluation of Breakdown Characteristics of Gas Insulated Switchgears for Non-standard Lightning Impulse Waveforms - Breakdown Characteristics for Non-standard Lightning Impulse Waveforms Associated with Disconnector Switching Surges." *IEEE Trans. Dielectr. Electr. Insul.* 3 (2008): 721-729. Web.

[21] Ueta G, Kaneko S, Okabe S. "Evaluation of Breakdown Characteristics of Gas Insulated Switchgears for Non-standard Lightning Impulse Waveforms – Breakdown Characteristics under Non-uniform Electric Field." *IEEE Trans. Dielectr. Electr. Insul* 5 (2008): 1430-1438. Web.

[22] Okabe S, Yuasa S, Kaneko S, Ueta G. "Evaluation of Breakdown Characteristics of Gas Insulated Switchgears for Non-standard Lightning Impulse Waveforms – Breakdown Characteristics for Non-standard Lightning Impulse Waveforms under Diverse Conditions." *IEEE Trans. Dielectr. Electr. Insul* 5 (2008): 1415-1423. Web.

[23] IEEE Standard Techniques for High-voltage Testing, IEEE Std. 4-1995, 1995. Web.

[24] Amendment to IEEE Standard Techniques for High-Voltage Testing, IEEE Std. 4a-2001, 2001. Web.

[25] Malik NH, Qureshi AH. "The Influence of Voltage Polarity and Field Non-Uniformity on the Breakdown Behavior of Rod-plane Gaps Filled with SF_6." *IEEE Transactions Electrical Insulation* 14 (1979): 327-333. Web.

[26] Monga S, Gorur RS, Hansen P, Massey W. "Design optimization of high voltage bushing using electric field computations." *IEEE Transactions on Dielectrics and Electrical Insulation* 6 (2006): 1217-1224. Web.

[27] Rodriguez D, Gorur RS, Hansen PM. "Effect of humidity on the breakdown characteristics of air in uniform field for the very low frequency (VLF) band." *IEEE Transactions Dielectrics and Electrical Insulation* 5 (2009): 1397-1403. Web.

[28] Rodriguez D, Gorur RS, Hansen PM. "Effect of humidity on the breakdown characteristics of air in non-uniform fields at 30 kHz." *IEEE Transactions Dielectrics and Electrical Insulation* 1 (2010): 45-52. Web.

[29] Howard Cohen E. "The electric strength of highly compressed gases." *Proceedings of the IEE-Part A: Power Engineering* 103 (1956): 57-68. Web

[30] Kuffel E, Radwan RO. "Time lags and the breakdown and corona characteristics in sulphur hexafluoride." *Proceedings of the Institution Electrical Engineers* 11(1966): 1863-1872. Web.